Respiratory motion management for proton and photon radiation therapy of small lung tumors

NILS OLOVSSON







Dissertation presented at Uppsala University to be publicly examined in Rudbecksalen, Dag Hammarskjölds Väg 20, Uppsala, Friday, 19 September 2025 at 08:30 for the degree of Doctor of Philosophy (Faculty of Medicine). The examination will be conducted in English. Faculty examiner: Associate Professor Liv Bolstad Hysing (University of Bergen).

Abstract

Olovsson, N. 2025. Respiratory motion management for proton and photon radiation therapy of small lung tumors. *Digital Comprehensive Summaries of Uppsala Dissertations from the Faculty of Medicine* 2169. 60 pp. Uppsala: Acta Universitatis Upsaliensis. ISBN 978-91-513-2545-3.

Lung cancer is globally recognized as the most common cause of cancer related death. The general prognosis is poor but for patients with early stage lung cancer very good local control can be achieved using stereotactic body radiation therapy (SBRT). These treatments are characterized by high doses to well defined targets delivered with high precision at a few treatment occasions. The common way of delivering these treatments is with X-ray photon beams. However, could these treatments be performed with proton therapy instead the theoretical dosimetric advantages of charged particle radiation therapy could be exploited to drastically reduce the dose given to healthy tissues. The very first proton therapies of cancer were given in Uppsala in the 1950s. Since 2015 modern proton therapy is available at the Skandion clinic in Uppsala but to this date no SBRT and no lung cancer patients have yet been treated which is addressed in this thesis.

When treating thoracic tumors the management of respiratory motion is of great importance and various strategies have been developed.

In this project, treatment planning methods for photon SBRT that take the respiratory motion into account were first evaluated and compared. Further, methods for treatment planning and evaluation were developed for proton SBRT. Additional imaging and treatment simulation strategies were used for the evaluation of the investigated treatment planning methods. Both treatments in free-breathing and in voluntary breath-hold were explored using the proposed methods.

The results indicate that robust treatment planning for this patient group can guarantee the desired target coverage for both proton and photon SBRT delivered in either free-breathing or breath-hold.

Further, proton therapy demonstrated a large reduction in dose to all surrounding organs which would further translate into clinical benefits for the patients treated with proton therapy compared with conventional photon radiation therapy.

Keywords: Radiation therapy, Lung cancer, Proton therapy

Nils Olovsson, Department of Immunology, Genetics and Pathology, Rudbecklaboratoriet, Uppsala University, SE-751 85 Uppsala, Sweden.

© Nils Olovsson 2025

ISSN 1651-6206 ISBN 978-91-513-2545-3

URN urn:nbn:se:uu:diva-564488 (http://urn.kb.se/resolve?urn=urn:nbn:se:uu:diva-564488)

"Any mass ten times its size and density should have been pulverized by that atomic barrage, but it wasn't."

> Planet Collision Experiment Zero (1996) Man or Astro-Man? Excerpt from Kronos (1957)

List of papers

This thesis is based on the following papers, which are referred to in the text by their Roman numerals.

- I Olofsson N., Wikström K., Flejmer A., Ahnesjö A., Dasu A. (2022) Dosimetric robustness of lung tumor photon radiotherapy evaluated from multiple event CT imaging. *Physica Medica*, 103; 1-10 doi:10.1016/j.ejmp.2022.09.007
- II Olovsson N., Wikström K., Flejmer A., Ahnesjö A., Dasu A. (2024) Impact of setup and geometric uncertainties on the robustness of free-breathing photon radiotherapy of small lung tumors. *Physica Medica*, 123; 103396 doi:10.1016/j.ejmp.2024.103396
- III Olovsson N., Wikström K., Flejmer A., Dasu A. (2025) Consistent robust treatment planning and displacement vector field editing for the probabilistic evaluation of radiotherapy of small lung tumors. Manuscript
- IV Olovsson N., Wikström K., Flejmer A., Dasu A. (2025) Comparison of proton and photon lung SBRT in free-breathing. *Manuscript*
- V Olovsson N., Wikström K., Flejmer A., Dasu A. (2025)
 Effects of breath-hold reproducibility uncertainty on proton and photon lung cancer radiotherapy.
 Manuscript

Reprints were made with permission from the publishers.

Contents

1	Introd	luction	11
	1.1	Lung cancer	11
	1.2	Stereotactic body radiation therapy (SBRT)	12
	1.3	Proton therapy	12
	1.4	Aim of the thesis	13
2	Radia	ation therapy of small lung tumors	14
	2.1	Radiation therapy and dose	
	2.2	Photon therapy with X-ray beams	15
	2.3	Particle therapy with proton beams	16
	2.4	Patient imaging and 4DCT	17
	2.5	Image registration	
	2.6	Management of respiratory motion and uncertainties	20
	2.7	Target volumes	22
	2.8	Dose prescription and reporting	
	2.9	Dose constraints and radiation toxicity	
	2.10	Treatment planning	
3	Treat	ment plan evaluation	28
	3.1	Patient image data	
	3.2	Evaluation image creation	
	3.3	Simulation of treatment uncertainties	
	3.4	Robust and probabilistic evaluation	33
4	Resul	Its and discussion	36
	4.1	Evaluation summaries and reporting	36
	4.2	Target coverage	
	4.3	Dose to the ipsilateral lung	
	4.4	Dose to mediastinal organs at risk (OARs)	
	4.5	Discussion	
5	Conc	lusions	43
6	Futur	e perspectives and prospects	44
7	Samn	nanfattning på Svenska	47
8	Ackn	owledgments	48
9	Biblio	ography	50

Abbreviations

General concepts.

4DCT Respiratory correlated Computed Tomography

AP Anterior-Posterior

BH Breath-hold

BHCT Breath-hold Computed Tomography

CC Craniocaudal

CT Computed Tomography
CTV Clinical Target Volume
DVF Displacement Vector Field
DVH Dose Volume Histogram

FB Free-breathing

ITV Internal Target Volume

LR Left-Right

NSCLC Non-Small Cell Lung Cancer

MR Magnetic Resonance

OAR Organ At Risk

PTV Planning Target Volume

RBE Relative Biological Effectiveness
SBRT Stereotactic Body Radiation Therapy

SPR Stopping Power Ratio

Dose metrics.

 $D_{
m mean}$ Mean dose received by anatomical volume $D_{
m max}$ Maximum point dose in an anatomical volume $D_{V\%}$ Lowest dose received by at least V% of the volume

 V_D Smallest volume receiving at least dose D

Treatment planning methods in papers I and II.

ISD Isodose photon plan

IRN Normalized isodose photon plan

FLU Fluence based photon plan

RB4 Robust optimized photon plan

1. Introduction

1.1 Lung cancer

Lung cancer is globally the most common cause of cancer-related death (Bray et al., 2024) and in Sweden there are 4500 new cases per year (Cancercentrum, 2025). Smoking is the largest risk factor and causes 80-90% of all lung cancers in Sweden (Cancercentrum, 2025) with other risk factors being work-related exposure, air pollution, and to some extent genetic factors (Holmqvist & Wagenius, 2024; Bray et al., 2024). Lung cancer is primarily diagnosed in the elderly and in Sweden the largest age group of new diagnoses is 70-79 years (Holmqvist & Wagenius, 2024).

Disease discovery can be made after an examination due to symptoms such as persistent cough or as an incidental finding. Diagnosis is subsequently established trough cytology or histology of biopsy material while local and metastatic spread are determined with positron emission tomography (Holmqvist & Wagenius, 2024). The treatment options depend on the disease characteristics where the staging based on tumor size, lymph node involvement, and presence of metastases as well as the histological distinction between small cell and non-small cell lung cancer (NSCLC) are the most important factors.

Despite progress with new and improved treatments a majority of the patients have a poor prognosis and the five-year survival for the disease in general is only about 24% (Holmqvist & Wagenius, 2024). However, patients with lower stage NSCLC, such as the one shown in Figure 1, can often be treated with curative intent using surgical resection or ablative radiation therapy and the five-year survival can be as high as 65% (Holmqvist & Wagenius, 2024).

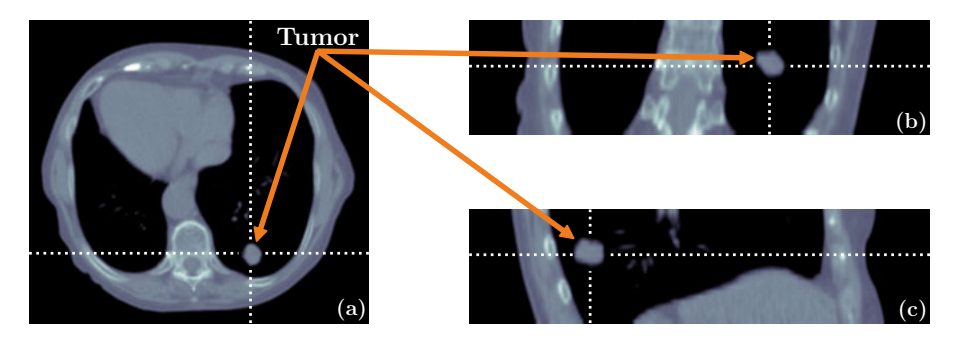


Figure 1. Computed tomography (CT) image of a patient with early stage lung cancer.

1.2 Stereotactic body radiation therapy (SBRT)

Primary NSCLC with lower staging, no suspected metastases, and contraindications or unwillingness for surgery are indications for radiation therapy with curative intent (Cancercentrum, 2025). Such tumors are treated with stereotactic body radiation therapy (SBRT) characterized by high doses delivered with high precision at three to five treatment occasions. SBRT using photon beams was pioneered in Stockholm, Sweden, in the 1990s (Lax et al., 1994; Blomgren et al., 1995) and has since demonstrated excellent local control on par with surgery (von Reibnitz et al., 2018). Further developments in computed tomography (CT), treatment planning techniques, dose computation algorithms, and on-board imaging capabilities have since cemented it as the radiation therapy standard of care for these patients.

Respiratory motion is a concern when treating thoracic tumors and several strategies to mitigate both breathing and other geometrical and radiological uncertainties are employed in the clinical workflow. However, the standard clinical method of respiratory correlated computed tomography (4DCT) underestimates the motion extent (Wikström et al., 2021) which will lead to dosimetric consequences that have been insufficiently studied.

Voluntary breath-hold (BH) is an attractive method for reducing the effects of respiratory motion to ensure the target position, compared with the conventional way of treating in free breathing (FB). Although BH is a tolerable mitigation method for many patients a large variation in the BH reproducibility has been reported and the dosimetric consequences of an inconsistently reproduced BH position in the SBRT setting are not well known (Aznar et al., 2023).

1.3 Proton therapy

The physical interactions of charged particles with matter give protons a finite range (Wilson, 1946). This advantage is directly translated into a drastically reduced dose in healthy tissues for proton therapy compared with conventional radiation therapy delivered with photons, as seen in Figure 2.

The first ever proton therapy treatment was performed in 1954 in Berkeley, USA, and concerned the ablation of the pituitary gland (Lawrence, 1957). Soon after, the first proton therapy treatment of human carcinoma was performed in 1957 in Uppsala, Sweden (Falkmer et al., 1962). Historically, these treatments were delivered at high energy physics laboratories and while contemporary proton therapy is based on the same physical principles modern treatment facilities have dedicated equipment to support the clinical application. Since 2015 patients in Sweden are treated at the Skandion proton therapy clinic in Uppsala.

Although theoretically advantageous, the finite range of the proton beam also makes the modality more sensitive to perturbations such as geometrical shifts compared with photon therapy. This sensitivity combined with the high

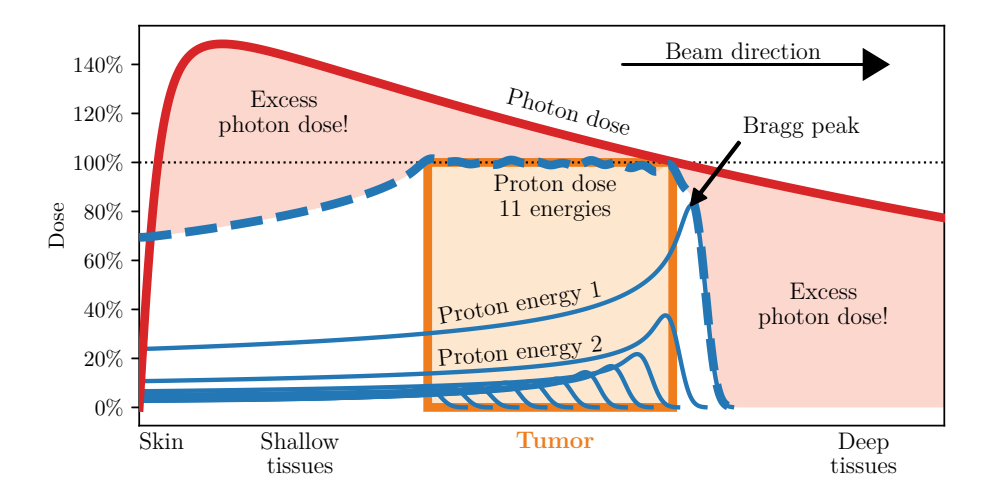


Figure 2. When comparing proton (Bortfeld & Schlegel, 1996) and photon (X.-J. Li et al., 2022) depth dose profiles an excess dose delivered with photons both to tissues in the entrance channel before the tumor and to deeper sited tissues behind it is seen. Notably, the finite range of a proton beam can be used to avoid dose deposition distal to the tumor location. The Bragg peak for the highest energy is highlighted.

precision requirements for SBRT has led to a very cautious clinical adoption of proton therapy for this type of treatment. Although proton SBRT and proton therapy for lung cancer are becoming more common internationally (Liu et al., 2024; Nakajima et al., 2024), to this date no SBRT and no lung cancer patients in Sweden have been treated with proton therapy which motivates the studies performed in this thesis.

1.4 Aim of the thesis

The aim of this thesis is to explore the impact of treatment uncertainties and respiratory motion on lung cancer SBRT dose distributions and how different motion management strategies in photon and proton therapy compare in this regard. The following aims were set:

- 1. Compare treatment planning methods for photon SBRT (papers I & II).
- 2. Develop and evaluate a treatment planning strategy for proton SBRT that accounts for uncertainties (papers III, IV & V).
- 3. Investigate respiratory motion management methods such as 4DCT based treatment planning (papers I IV) and BH (papers III & V).
- 4. Quantify the dosimetric effects of the uncertainties associated with respiratory motion (papers I IV), BH reproducibility (papers III & V), and patient positioning (papers II V) in lung cancer photon and proton SBRT.

2. Radiation therapy of small lung tumors

2.1 Radiation therapy and dose

Shortly after the discovery of X-rays by Wilhelm Röntgen in 1895 radiation was used to treat superficially located tumors. Today, half of all cancer patients receive radiation therapy as part of their treatment and 30% of all cured cancer is attributed to radiation therapy (Cancerfonden, 2023).

In external beam radiation therapy the radiation source is outside the patient. The radiation passes through the patient body while losing and depositing energy primarily through interactions with electrons. These interactions induce ionizations, which when they occur in the cell nucleus cause damage to the DNA of the irradiated cell. If the damage is severe enough it will stop the cell from proliferating, effectively killing it, which is the goal with irradiating tumors.

However, healthy tissues are unavoidably also irradiated which leads to treatment side effects with more or less severe complications. Radiation therapy always aims to maximize the cell killing effect in the tumor while keeping the risk of complications as low as possible. This is achieved by optimizing the dose distribution in and around the target, e.g. through the use of proton therapy and by irradiating from several directions as seen in Figure 3. The treatments are further fractionated such that they are delivered at several occasions. This allows for normal tissue cells to repair and it also promotes tumor cell killing through cell cycle phase redistribution and re-oxygenation (Withers, 1975). All treatments investigated as part of this thesis and presented in papers I - V were hypo-fractionated SBRT to be delivered in three fractions, every other day according to current treatment protocols (Guckenberger et al., 2017).

Absorbed radiation dose for prescribing, recording, and reporting is quantified in Gray (Gy), defined as 1 Joule per kg. A radiation therapy treatment plan is largely characterized by its three-dimensional dose distribution. It can be further summarized into dose volume histograms representing the frequency distribution of various dose levels in anatomical structures. In particular, cumulative dose volume histograms (DVH) are used to describe how large a fraction of the volume receives a certain dose. Several DVH examples are shown in Figure 3 where the dose distribution of a proton therapy plan is compared with one of a photon therapy plan, as studied in papers III and IV.

Descriptive quantities derived from the dose distribution and calculated per anatomical structure are used to set dose prescriptions and tolerance limits. For example the lowest dose, $D_{V\%}$, given to at least V% of the volume of some anatomical structure or alternatively by the size or fraction of the volume, $V_{D\,\mathrm{Gy}}$, receiving at least the dose $D\,\mathrm{Gy}$.

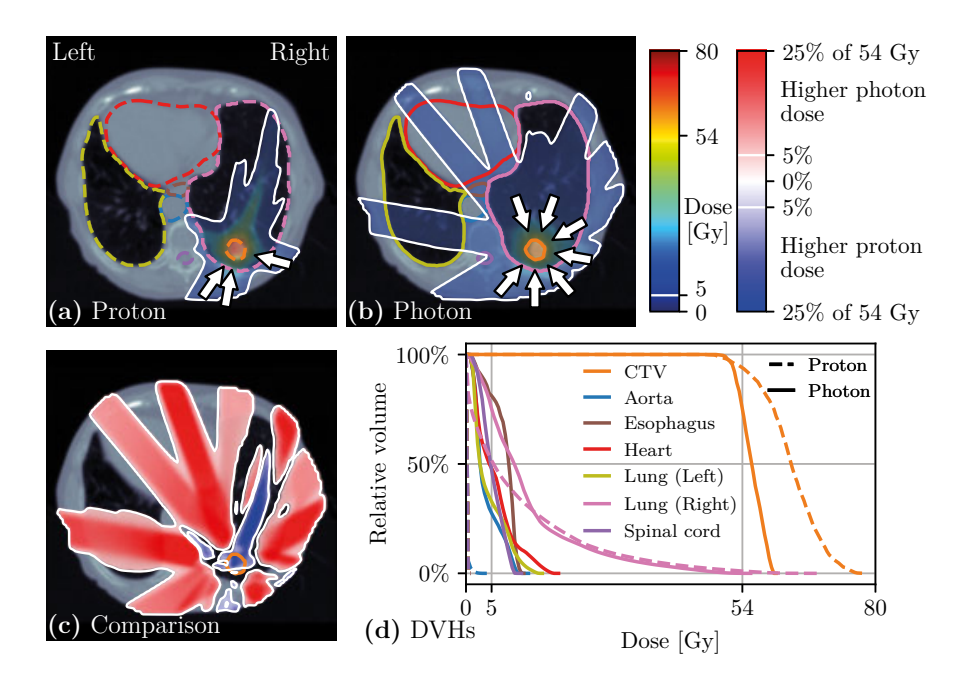


Figure 3. Treatment planning, nominal, dose distributions for a (a) proton plan with three beam directions and a (b) photon plan with seven beam directions, indicated by the white arrows. The proton plan spares the entire left side of the body and the mediastinum including the heart which can be seen in the difference in dose distributions (c) and when comparing the dose volume histograms (DVHs) (d). Doses below 5 Gy in (a) and (b) and differences below 5% of the prescription dose of 54 Gy in (c) are not shown.

2.2 Photon therapy with X-ray beams

Early radiation therapy was administered with keV photon beams from X-ray tubes or with radioactive isotopes applied directly at superficial tumors. Later dedicated devices used higher energy gamma sources such as cobalt-60 enclosed in shielding with openings that allowed stereotactic treatments of deep-seated, intra-cranial, tumors (Larsson et al., 1974).

While cobalt sources are still used to some extent, modern radiation therapy is mostly delivered with MeV X-ray photon beams produced with linear accelerators. Electrons are accelerated to a specific energy, typically between 6 and 18 MeV, and directed at a target with high atomic number such as tungsten which produces a beam of high-energy bremsstrahlung X-rays. The beam is shaped downstream by a pair of *jaws* and further collimated orthogonally by two sets of opposing *leaves*.

In addition, the collimator-equipped treatment head can rotate around the patient to deliver the beam from any circular angle. The machine can be equipped



Figure 4. A treatment room for photon therapy at the Uppsala university hospital. The gantry mounted linear accelerator and treatment head can rotate around the table on which the patient lies. Perpendicular to the beam direction is an imager capable of cone-beam CT. In the ceiling there are three surface scanning cameras that aid with the patient positioning.

with on-board imaging perpendicular to the beam direction which enables patient positioning based on internal anatomy. The position of the patient in relation to the rotational iso-center is adjusted by a motorized treatment table, seen in Figure 4. Modern irradiation techniques make use of these machine attributes in concert to deliver a very precise dose to the target.

2.3 Particle therapy with proton beams

The majority of radiation therapy treatments are delivered with photons but also electron beams and beams of light ions such as protons, helium, and carbon are in clinical use.

Unlike photons, charged particles such as protons have a finite range with an energy deposition per track length that increases along the track until it dramatically achieves a maximum, the so-called Bragg peak, see Figure 2. The finite range and the Bragg peak enable dose delivery to the target while sparing distal tissues, which is not possible with photon therapy (Wilson, 1946). The proton beam range is proportional to its initial energy requiring that multiple energies are used to spread the Bragg peaks over the tumor. A typical maximum energy for clinical proton facilities is 230 MeV which corresponds to a range of 32 cm in water and allows treating deep seated targets in most patients.

Proton beams of desired energies are produced by the acceleration of protons in either a synchrotron or a cyclotron. From the accelerator the protons travel

through a beam line equipped with magnets that focus and direct them to the treatment room. Modern facilities are equipped with gantries that can rotate around the patient to deliver the beam from different angles just as for photon therapy, see Figure 5. The dose is finally delivered with narrow pencil beams that are controlled with magnetic scanning techniques to laterally cover the tumor in a painting-like manner. The in-plane pencil beam scanning covers a layer of the tumor with dose with its depth controlled by varying the energy from a maximum to a minimum value, as illustrated in Figure 6. The dynamics of this treatment delivery method was considered in the BH studies in papers III and V.

The biological effect of the deposited radiation energy depends largely on how dense clusters of damage the ionization causes. The variation in biological effect per dose for various radiation types is empirically quantified by the relative biological effectiveness (RBE) defined as the dose ratio compared to a reference photon radiation yielding equal cell killing effects. Different RBE models have been proposed, however in clinical practice a constant multiplicative value of 1.1 is used (Paganetti et al., 2002, 2019) and so also in this thesis throughout papers III - V. All reported proton dose distributions were thus converted using this constant factor as Gy (RBE) but are for the sake of briefness reported as Gy in this report.

Proton beam therapy is used for the treatment of most tumor sites, with some special emphasis on intra-cranial and intra-spinal pediatric tumors (Paganetti, 2019). However, the adoption of proton therapy in lung cancer radiation therapy has been slow, primarily due to the uncertainties associated with respiratory motion and large differences in tissue density. As such, no patients with lung tumors have yet been treated with proton therapy in Sweden which is addressed by this thesis.

2.4 Patient imaging and 4DCT

In radiation oncology, medical imaging is used for disease detection and staging, treatment planning, patient positioning, and during follow up examinations. A multitude of imaging modalities are employed for this purpose, ranging from CT, positron emission tomography, and magnetic resonance (MR) to surface scanning.

The radiation therapy workflow begins with the acquisition of one or more CT images of the patient and this can be considered the most important image modality in radiation therapy (Goitein et al., 1979). Motion artifacts are minimized with breath-hold computed tomography (BHCT) where the patients hold their breath either with a deep inspiration or at an exhale position during imaging. Such BHCTs were used as reference geometry for the tumor tracking in paper I and as basis for the BH studies in papers III and V.



Figure 5. A treatment room for proton therapy at the Skandion clinic in Uppsala. In contrast to the linear accelerator seen in Figure 4, only the very final part of the proton beam line is visible in the form of the gantry mounted treatment head that can rotate around the patient. In the ceiling there are three cameras for surface scanning to help with the patient positioning, similar to the photon therapy treatment room in Figure 4.

For lung cancer the tumor motion due to breathing is further quantified using 4DCT (Vedam et al., 2003; Ford et al., 2003). Phase images are reconstructed from over-sampled CT image data acquired simultaneously with a respiratory signal that is used to sort the data into bins according to their respiratory phase or amplitude, see Figure 7. A clinical 4DCT typically consists of 10 reconstructed volumetric CTs, each corresponding to a phase position on the respiratory cycle or to the amplitude of the respiratory signal. The respiratory signal can be measured by the tidal volume of a spirometer, with surface scanning, from the position of a fiducial marker on the abdomen, or from a bellows or belt device that captures the motion of the chest or abdomen. The 4DCT can also be reconstructed using self-sorting based on a surrogate signal derived from the images themselves. 4DCT is an essential tool for motion management and treatment planning of thoracic tumors and such 4DCTs were used for all treatment planning and as basis for the evaluations in the FB studies in papers I - IV.

There are however several limitations to 4DCT. Since the imaging time is limited and only part of the patient is covered by the CT detector array at one time there is a risk of under sampling or completely missing certain phase positions at some image slice locations. Such a miss will result in an image artifact that can be seen as a discontinuity or cropping of the anatomy. Because the risk of under sampling is greater for more extreme positions these may not be captured at all in the reconstructed 4DCT and the full extent of

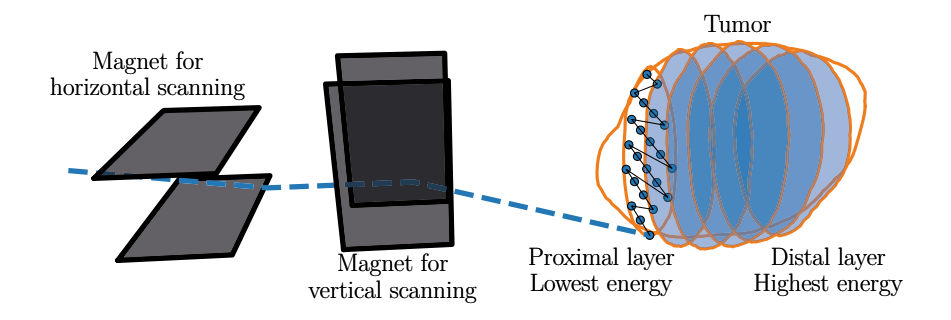


Figure 6. Pencil beam scanning is used to paint the target with protons. The particles are steered by a set of horizontal and vertical magnets while the depth layer position is determined through energy selection.

the respiratory tumor motion will be underestimated (Wikström et al., 2021). Further, the 4DCT only reconstructs one breath without any of the variations in breathing that occur both within a single treatment fraction and between the treatment fractions. At best, the 4DCT represents an artificially reconstructed, arbitrary, single breath at the time of the imaging session. The dosimetric consequences of these limitations were investigated in this thesis in papers I-IV using cine-CT and image registration methods that are further described in Sections 3.1 and 3.2.

2.5 Image registration

Image registration is the process of finding a transform that maps the content of a *moving* image such that it matches the content of a *fixed* image as reference (Barnea & Silverman, 1972; Sotiras et al., 2013). The transform can represent either a rigid body motion consisting of translations and rotations or more complex correspondences that include deformations that allow for objects in the image to change shape, such as the example in Figure 8. The transform is found by solving an optimization problem that maximizes a similarity metric between the fixed and the transformed moving image.

The obtained transform is used for mapping anatomical structures from one image to another and in the context of lung cancer radiation therapy this is used to estimate the tumor motion in 4DCT. By inverting the transform it can further be used to map radiation dose computed on one image back to a reference geometry to allow for dose accumulation. A transform is described by a displacement vector field (DVF) quantifying the position shifts of elements between the images.

Both rigid and deformable image registration was used in this thesis. Deformable image registration mapped structures in the treatment planning process in papers I - V. Rigid image registration was used in the treatment plan

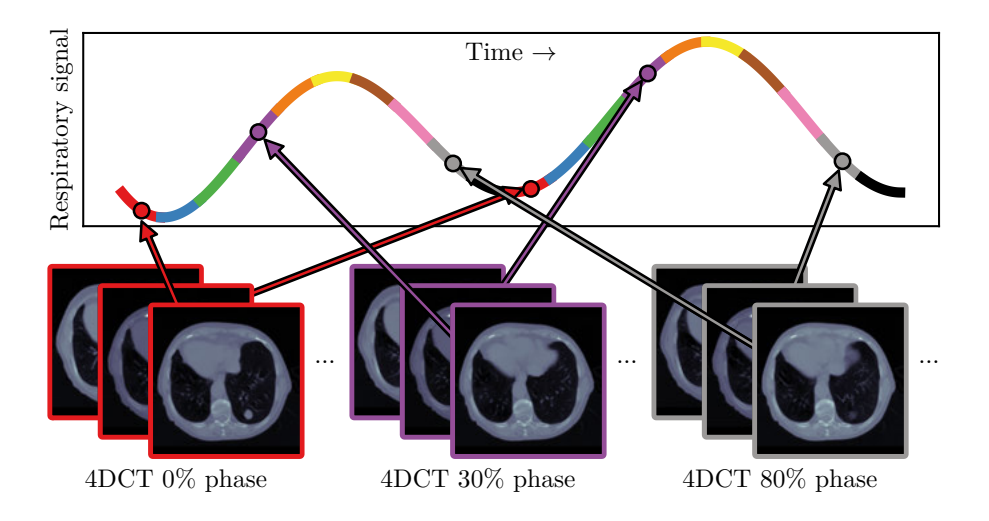


Figure 7. A phase sorted 4DCT is reconstructed from image data at different time points but corresponding to the same respiratory phase position. Here assembled into 10 phase image volumes as indicated by the colors. The respiratory motion is periodic in nature but can still be irregular and have a varying amplitude which can give rise to artifacts in the reconstructed phase image volumes and an underestimation of the motion extent (Wikström et al., 2021).

evaluation to find tumor positions in cine-CT images and for dose accumulation in papers I and II, as further described in Section 3.1. Both rigid and deformable (Rueckert, 1999) image registrations were used for this same purpose in paper IV with a DVF editing method introduced in paper III and further described in Section 3.2.

2.6 Management of respiratory motion and uncertainties

Radiation therapy of lung cancer is subject to geometrical and radiological uncertainties (Schwarz et al., 2017), primarily due to respiratory motion of the tumor that in extreme cases can be as large as a few centimeters. The motion amplitude varies greatly between patients and also across different regions in the lungs with the largest amplitudes found in the lower lobes close to the diaphragm (Seppenwoolde et al., 2002). The management of respiratory motion mitigates the impact on the treatment through different active or passive strategies (Keall et al., 2006; H. Li et al., 2022).

Passive strategies consist of methods in which the motion is confined e.g. by abdominal compression and/or accounted for at the planning stage e.g. with an additional motion-encompassing margin around the target volume, further described in Sections 2.7 and 2.10. The respiratory motion is estimated with 4DCT and the assumption in the 4D treatment planning (Wolthaus et al., 2008)

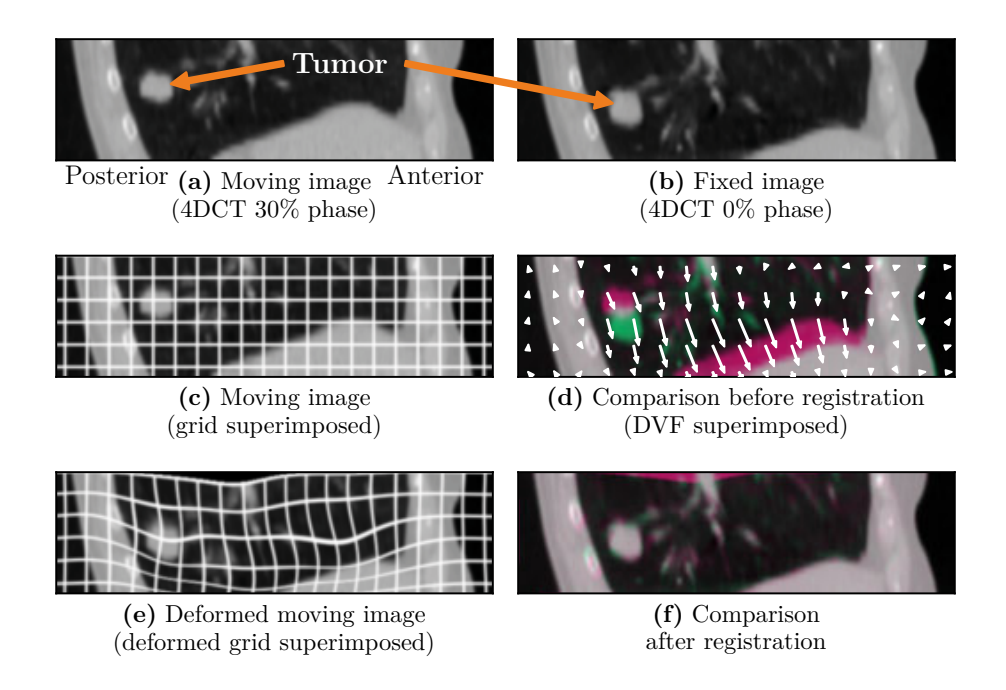


Figure 8. Image registration finds a transform that maps one image (a) to another (b). The effect of the transform can be highlighted by superimposing a grid on the original (c) and on the deformed image (e). Two images can be visually compared with image fusion where discrepancies in pixel intensity are seen as a pink or green color, (d) and (f). The resulting transform can be represented by a displacement vector field (DVF) which can be visualized as a set of arrows that indicate the local position displacements (d).

is that the patient will exhibit the same breathing pattern throughout the whole treatment. Treatment planning based on 4DCT was investigated and evaluated in this thesis in papers I - IV.

Active strategies imply that the breathing of the patient is controlled or additional technological devices for real-time monitoring and motion compensation are used. The real-time motion information is then used to either track the target volume to continuously deliver the dose or to gate the treatment such that the beam is active only when the target has a position within a predefined gating window, e.g. in voluntary BH (Willett et al., 1987; Hanley et al., 1999). Although the use of active BH eliminates the respiratory motion there still remains an uncertainty in the reproducibility of the tumor position that needs to be considered (Josipovic et al., 2019; Hoffmann et al., 2023). The use of BH and the effects of variation in the reproducibility were investigated in this thesis in papers III and V.

Errors in the setup positioning of the patient on the treatment table is another source of geometric uncertainty. These errors are minimized by laser-guidance

or body surface scanning and further fine-tuned using on-board imaging such as portal imaging, fluoroscopy or, cone-beam computed tomography, for some of which the equipment is visible for in Figures 4 and 5. With these techniques the patient setup error can be reduced to just a few millimeters (W. Li et al., 2011), but the residual difference will still impact the dose distribution for each treatment fraction. Patient positioning errors were included in the treatment planning and evaluations performed as part of this thesis in papers II - V.

In addition, proton therapy is also affected by uncertainties in the stopping power ratio (SPR) estimated from the planning CT since it influences the predicted range of the protons. This uncertainty can be reduced with the use of dual-energy CT but remains of great importance in lung cancer treatments because of the large differences in density between lung and tumor tissues (B. Li et al., 2017). Uncertainty in SPR was considered in all proton therapy plans investigated in this thesis, papers III - V.

All these treatment uncertainties are divided into systematic errors that occur during treatment preparation and *random* errors that occur during treatment delivery (Van Herk et al., 2000). This distinction was explicitly taken into consideration in papers III - V.

2.7 Target volumes

Several target volumes are defined for the use in treatment planning by the International Commission of Radiation Units and Measurements, ICRU (Gregoire et al., 2010; Brandan et al., 2014). For SBRT treatments of lung cancer at the Uppsala university hospital the clinical target volume (CTV) is directly delineated on the planning CT image. A motion-encompassing internal target volume (ITV) is further created from the union of the CTV in all phase images of the 4DCT or from a delineation of the volume with tumor presence in a maximum intensity projection image. An additional margin to account for patient positioning errors and other uncertainties is added around the ITV to create the planning target volume (PTV) (Van Herk et al., 2000). These three target volume concepts are illustrated in Figure 9.

The CTV was used in the treatment planning and evaluation in all studies that are part of this thesis while the ITV was used in paper I and the PTV in paper II. Although the ITV and PTV concepts can be adapted for proton therapy treatment planning of lung tumors (Kang et al., 2007; Langen & Zhu, 2018) they come with several limitations (Unkelbach et al., 2018) and were therefore not used in any of the proton therapy studies in this thesis.

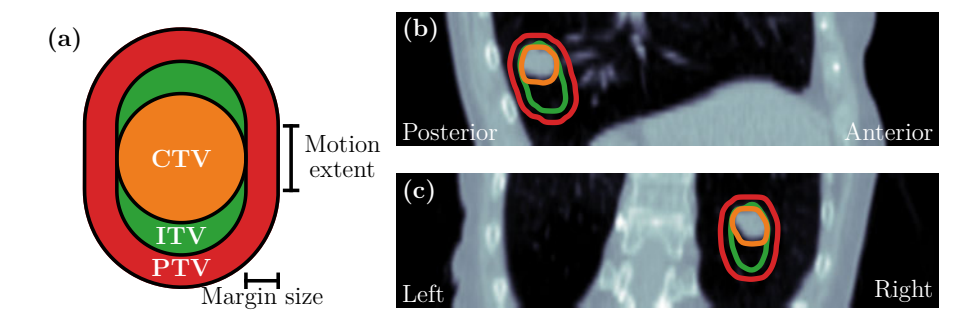


Figure 9. The clinical target volume (CTV) was defined as the visible tumor. The internal target volume (ITV) was further defined from the CTV swept by the respiratory motion extent by taking the union of the CTV in the ten 4DCT phases. Finally a 5 mm margin was added to account mainly for patient positioning uncertainty which formed the planning target volume (PTV). The patient example shows a 4DCT at the 30% phase with the target volumes visible in the (b) sagittal and (c) coronal planes.

2.8 Dose prescription and reporting

Treatments of small lung tumors are delivered with high doses in few fractions using SBRT (Lax et al., 1994; Blomgren et al., 1995). Dose prescriptions are typically set such that the tumor is given at least a minimum dose by prescribing a near isodose, e.g. $D_{98\%}$, to the PTV. However, since the PTV periphery for small lung tumors is located in lower density lung medium there is a loss of charged particle equilibrium which leads to an uncertain lower dose for the CTV. Since the dose computation algorithms clinically available when SBRT for small lung tumors was introduced did not account for these phenomena (Battista, 2019), dose prescriptions to PTV can yield large errors in CTV dose (Lebredonchel et al., 2017), which was explored in papers I and II.

Prescribing a mean or median dose to the CTV based on algorithms that account for electron transport (i.e. collapsed cone (Ahnesjö, 1989), Monte Carlo (D E Raeside, 1976; Andreo, 1991), or grid-based Boltzmann equation solvers (Bush et al., 2011; Fogliata et al., 2011)) together with appropriate field margins to ensure PTV irradiation has been shown to give more consistent treatments and harmonize the delivered dose to the tumor between patients and institutions (Bibault et al., 2015; Leung et al., 2020; de Jong et al., 2020). As such, a CTV $D_{50\%}$ = 54 Gy delivered in three fractions has been suggested for lung tumor SBRT (Bibault et al., 2015; Baumann et al., 2018).

This prescription was used in all studies presented in papers I - V that are part of this thesis. Further, it was also used as the primary dose metric to report when evaluating and comparing treatment plans. Traditional ITV and PTV based dose prescriptions were also used for comparison in some of the treatment planning methods investigated in papers I and II respectively. In these two studies dose to the ITV respectively to the PTV were reported as well.

2.9 Dose constraints and radiation toxicity

The irradiation of normal tissues around the target can result in toxicity that ranges from life-threatening to a temporary lowering of the quality of life of the patient. Toxicity is commonly divided into acute and late manifesting effects where the second of these two often is to be considered more severe as it describes persistent damage that may never properly heal for the rest of the patients life. Further, radiation exposure is also associated with a higher risk of developing secondary cancers. Therefore, dose received by the organs at risk (OAR) needs to be kept at a minimal level. For lung cancer the main OARs are lung, heart, esophagus, and spinal cord. The treatment planning performed in this thesis used widely adopted dose constraints for these OARs in the SBRT setting (Benedict et al., 2010; Timmerman, 2022).

Radiation exposure of the lungs is associated with pneumonitis, a lung inflammation, which can manifest from the time of treatment up to a few months after. A later and more severe side effect is lung fibrosis which can occur a year or more after treatment (Cancercentrum, 2025). The ipsilateral lung $V_{20~\rm Gy}$ and $V_{5~\rm Gy}$ are used to manage the risk for these side effects (Khalil et al., 2015) and were reported for all studies in this thesis.

A radiation dose to the heart is mostly associated with late effects such as a higher probability of heart disease years after the treatment. The available data are primarily derived from studies of late effects from treatments of patients with breast cancer or Hodgkin's lymphoma that have better overall prognosis and time of survival than lung cancer. For breast cancer patients it has been suggested that the risk of a cardiac event increases by 7% per Gy in mean heart dose. (Darby et al., 2013). Hence, the mean dose, $D_{\rm mean}$, of the heart was reported in papers III - V. However, the heart volume was truncated or not present at all in some patients in the cohort due to limited field-of-view in the CT images. Thus providing a conservative estimate of the heart $D_{\rm mean}$ in the patients with the heart visible in the CT images.

Esophagitis is an inflammation of the esophagus that can cause pain, difficulties with swallowing, and nutrition problems. More severe is perforation of the esophagus that greatly reduces the quality of life and increases mortality.

The spinal cord is considered to be relatively radioresistant (C. Joiner, 2025) but due to the extreme impact of neuropathies such as paraplegia on the quality of life, reducing its exposure should be highly prioritized. Thus any but especially high doses to the spinal cord should be avoided.

Since both the esophagus and the spinal cord are serial OARs, as opposed to being a parallel OAR such as the lung, the maximum doses, $D_{\rm max}$, received by these two were reported for the studies in papers III - V. High doses to the great vessels should also be avoided as they are associated with aneurysms (Benedict et al., 2010; Timmerman, 2022). As such, $D_{\rm max}$ to the aorta was reported in the studies in papers III - V.

Additional adverse effects may include radiation-induced fractures of the ribs and skin symptoms ranging from irritation and redness to necrosis. Although the skin dose was considered in the treatment planning in papers II - V it was not further reported in any part of this thesis. Irradiation of breast tissue should also be avoided and this was minimized by choice of gantry angles in all studies performed during this thesis.

2.10 Treatment planning

Various strategies involving the use of 4DCT for treatment planning have been proposed, including methods using mid-position of the target and the ITV (Wolthaus et al., 2008). In margin-based 4D treatment planning the patient positioning uncertainty is managed with the addition of a PTV margin around the ITV and a prescription dose or other conformity criteria is defined for the PTV as described in Sections 2.7 and 2.8. The treatment planning system finds treatment delivery parameters by solving an optimization problem such that target coverage is ensured while dose constraints to OARs are maintained. In papers I and II different margin-based planning methods were investigated and compared for photon SBRT.

Although margin-based planning methods are more common, scenario based robust planning primarily introduced in the context of particle therapy is available in many commercial treatment planning systems (Fredriksson et al., 2011). In 4D robust SBRT planning the dose is prescribed to the CTV and its delineation in multiple phases of the 4DCT is used to accommodate for the respiratory motion while discrete position perturbations are employed to account for patient setup uncertainty.

Typically two perturbation steps are taken along each cardinal axis which together with the zero shift give seven positions. If all ten respiratory phase images in the 4DCT are used in the robust optimization this give a total of $7 \times 10 = 70$ plan scenarios to optimize in the case of photon therapy. For proton therapy the range uncertainty must also be considered which is typically done with two additional perturbations of the SPR for a total of $3 \times 7 \times 10 = 210$ plan scenarios. The robust optimizer then attempts to find a plan that fulfills the planning criteria for all plan scenarios. In the minimax robust optimization strategy (Fredriksson et al., 2011) the plan is adjusted by re-optimizing it according to the worst dose distribution out of the current plan scenarios. The 4D robust planning investigated in paper I used all ten phase images in the 4DCT but without any patient shifts. In order to reduce the number of plan scenarios and reduce the computational time a smaller subset of the 4DCT phase images can be used in the optimization process. Such subsets of images were used in the robust treatment planning in papers II - IV together with patient positioning shifts and SPR perturbations for the proton therapy plans.

In papers I and II four different photon therapy treatment planning methods were evaluated and compared. They were denoted as a SBRT ITV/PTV strategy with dual criteria of a central higher dose and ITV/PTV isodose (ISD), a normalization of the former to a dose to the CTV (IRN), a conformal method based on homogeneous fluence to the ITV/PTV (FLU), and robust 4D planning to the CTV (RB4).

Perturbation settings for robust planning are calculated from the error distributions of the considered treatment uncertainties (Buti et al., 2019). In paper III this approach was used to calculate parameters for the FB treatments investigated in paper IV and the method was further expanded upon in the same study and used for the BH treatments investigated in paper V.

All treatment plans in papers III, IV, and V further made use of robust evaluation in the planning process where each plan was normalized such that the worst case evaluation scenario fulfilled the prescription dose. A summary of all treatment plannings methods investigated in this thesis is found in Table 1.

In paper IV 4D robust treatment planning was used for the investigation of FB photon and FB proton treatments. In paper V robust treatment planning was used for the investigation of BH photon and BH proton treatments. For the BH proton plans to be realistically deliverable, the beams were split into two sub-beams if they contained more than ten energy layers. In the study three BH treatment planning methods per modality were investigated and compared for a total of six plans per patient. However in this thesis summary only the results for the robust 3D BH proton and photon treatment plans, labeled as proton_{3D-BH} and photon_{3D-BH} in paper V, are reported. A comparison of a FB proton and a BH proton dose distribution is shown for a patient with large respiratory motion in Figure 10.

All treatment planning and all dose computations were performed in a research version of the RayStation treatment planning system (RaySearch Laboratories AB, Stockholm, Sweden). All photon dose computations were performed with the collapsed cone algorithm and all proton dose computations with Monte Carlo.

Table 1. Treatment planning strategies and methods investigated throughout the thesis. *The treatments plans in paper I did not include patient setup uncertainty. † Paper III only reports results for a single patient.

		Photon only		Photon and proton		
		I*	II	III^{\dagger}	IV	V
	Margin based,					
	optimized or fluence based	✓	✓			
Free breathing	(photon)					
ree ath	Robust optimized		((
F	(photon)	v	•	\ \ \	•	
	Robust optimized					
	(proton)			V	V	
	Robust optimized					
Breath	(photon)			V		V
	Robust optimized					(
	(proton)			V		V

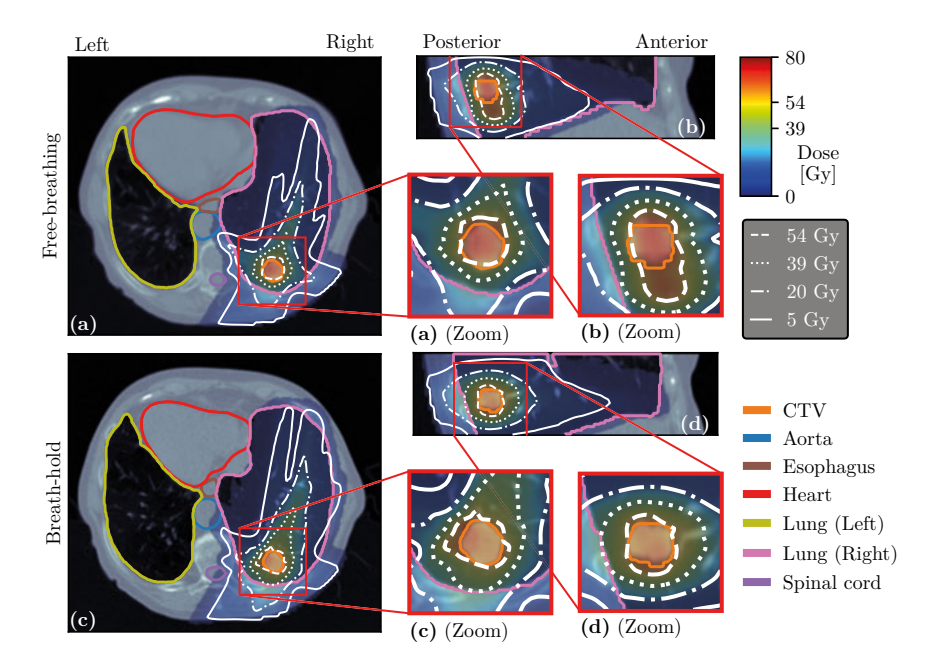


Figure 10. Comparison of proton treatment plans in free-breathing (FB) and breath-hold (BH) for a patient with large respiratory motion. To account for the respiratory motion, see e.g. Figure 9, a large elongated volume of the lung would have been irradiated (b). By treatment planning for BH gated delivery this volume was reduced along the craniocaudal direction (d) compared with the FB treatment plan (b). However, accounting for the population based BH reproducibility uncertainty lead to a larger irradiated area in the transverse plane, as seen when comparing (a) with (c) in the area around the clinical target volume (CTV).

3. Treatment plan evaluation

3.1 Patient image data

Image data from 14 patients with early stage lung cancer previously acquired as part of a motion analysis study (Wikström et al., 2021) were used throughout this thesis. These data consisted of planning images from BHCT and a 4DCT with ten respiratory phase images, and in addition to that a total of 300 cine-CT images per patient acquired at three occasions. At each occasion, 100 images were collected during eight minutes resulting in image sets labeled A, B, and C, see Figure 11. In order to investigate the dosimetric consequences of the limitations in 4DCT, the cine-CTs were used to estimate the FB tumor positions for the treatment plan evaluations.

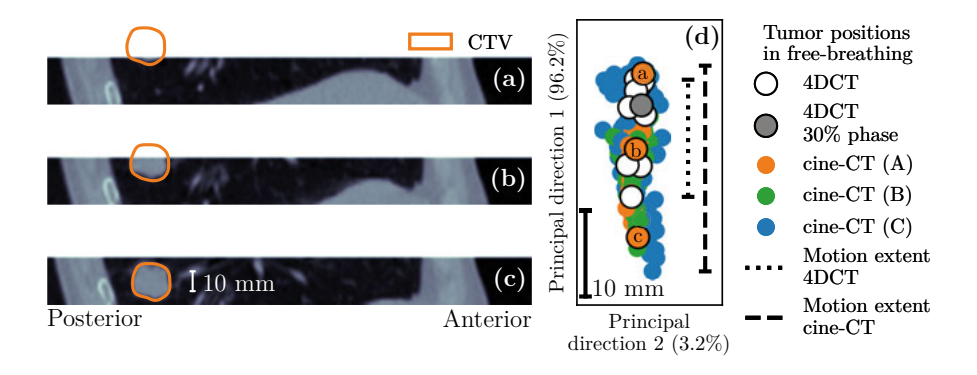


Figure 11. The clinical target volume (CTV) positions in free-breathing were found by rigid image registration of the tumor volume to the 300 cine-CT images. Depending on the motion extent and tumor size the tumor could occasionally be almost completely outside of the imaging field-of-view as seen in (a). The resulting motion extent as observed in the cine-CT was larger than the motion observed in 4DCT for all 14 patients included in this thesis, as seen for this particular patient in (d) were all tumor positions have been projected on the two principal motion directions. The percentages indicate the explained variance of the motion along that direction. The tumor positions in the cine-CT images (a), (b), and (c) are indicated in (d).

However, the geometric coverage of the detector arrays in the used CT scanner, Philips Brilliance[®] CT Big Bore 16 slice, limited the cine-CT volume thickness to only 24 mm which impeded the direct usage of these images for dose evaluation studies, see Figure 11. Additional processing with two methods

developed in papers I and III was therefore performed to create evaluation images that were used throughout all FB studies in this thesis, papers I - IV. An alternative method was further used to create additional BHCT images with tumor position perturbations that simulated errors in BH reproducibility.

In this patient cohort the CTV size varied between 1.3 cm³ and 21.5 cm³, the motion amplitude as observed in the 4DCTs varied between 1.4 mm and 16.8 mm, and between 7.4 mm and 41.6 mm as observed in the cine-CTs. The extents of the respiratory motion of the lung tumors were found to be underestimated in the 4DCTs for all 14 patients. Per patient values are reported in paper I and the patient used as example throughout this report e.g. in Figures 9, 10 and 11 had a CTV size of 3.8 cm³, a motion extent in the 4DCT of 14.4 mm and a motion extent in the cine-CTs of 24.1 mm. Although some of the patients in actuality were treated with abdominal compression to suppress the respiratory motion all images used in this thesis were acquired without any such devices, thereby showing cases more extreme than typically observed clinically.

3.2 Evaluation image creation

The dosimetric effects of respiratory motion is commonly evaluated with the same 4DCT that was used during treatment planning and then the limitations, as described in Section 2.4, of these images apply. In this thesis improved methods based on sets of evaluation images derived from cine-CT were used.

Since the cine-CT images themselves were too small to be used for dose calculations they were instead used for finding the tumor positions which were then used to shift the tumor around in a larger image volume that permitted dose computation. In paper I, rigid image registration was used to find the FB positions of the tumor in all cine-CTs, as is illustrated for one patient in Figure 11.

Subsequently, evaluation images were created by cropping the image region around the CTV in the BHCT and superimposing it at the cine-CT position on the 4DCT phase image that best matched this new position. These evaluation images were used in the treatment plan evaluations in both papers I and II. Although this method was accurate for the dose accumulation in the CTV the discontinuity at the edge of the cropped volume prevented dose to be accurately accumulated in the lung. And, further, since no image registrations were available between the 4DCT phase images, dose accumulation in the other OARs was also not possible.

This limitation was addressed in the improved method developed in paper III and further used in paper IV. In this method, deformable image registrations between the 4DCT phase images were first performed which allowed for dose accumulation in the OARs. Further, the tumor was shifted according to its position in the cine-CT using a Poisson DVF editing technique (Perez et al.,

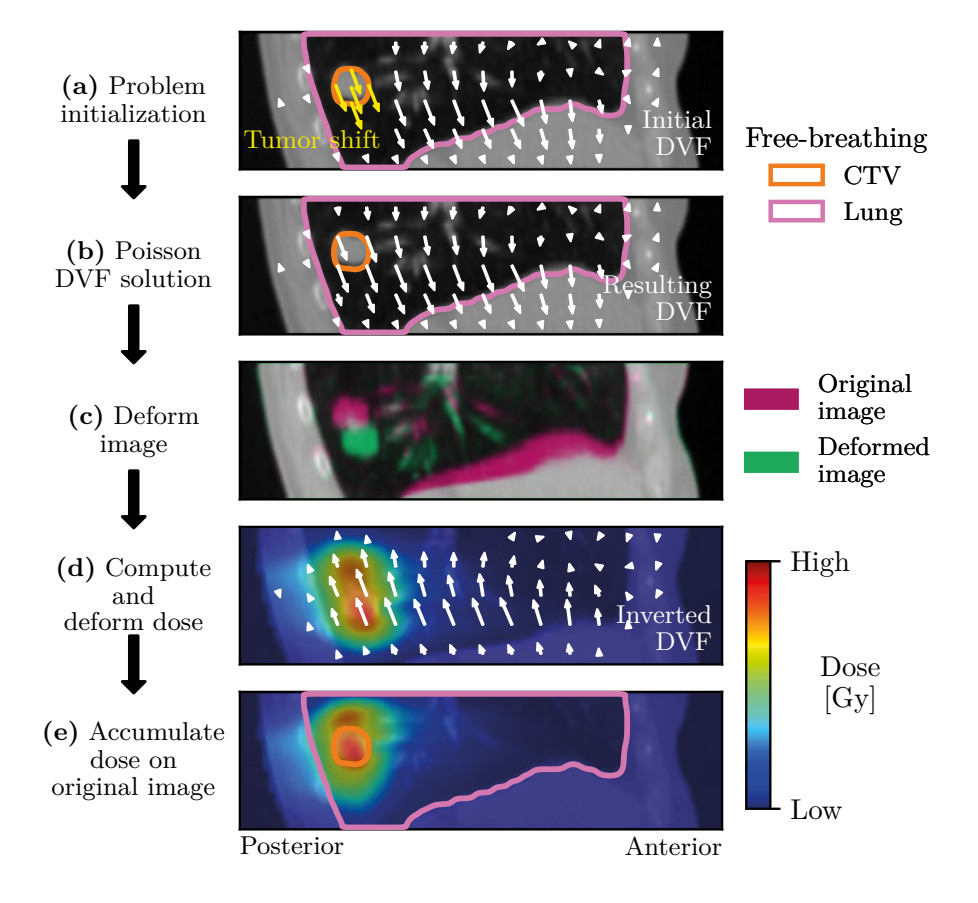


Figure 12. Free-breathing images for the probabilistic evaluation in paper IV were created using a Poisson displacement vector field (DVF) editing method introduced in paper III. (a) The clinical target volume (CTV) shifts were determined from the cine-CT images and the initial DVFs were set from deformable image registration of the 4DCT phase images. (b) The resulting DVF transform was used to create an evaluation image (c) which could be used for dose computations. (d) The DVF transform was inverted to allow for dose accumulation (e) on the original reference 4DCT phase image. This DVF processing procedure was performed for all 300 cine-CT images for all 14 patients in the cohort used in the studies in this thesis.

2003), as illustrated in Figure 12. This technique was used to locally alter the deformable image registration DVF transform around the CTV into a resulting DVF transform with correct tumor position. Finally, this transform was inverted to allow for dose accumulation in the CTV and all OARs in the treatment plan evaluations in papers III and IV.

A similar technique for local Laplacian deformations (Sorkine et al., 2004) was also developed in paper III and further used to create BH images with simulated reproducibility errors. These BHCT images with shifted tumor

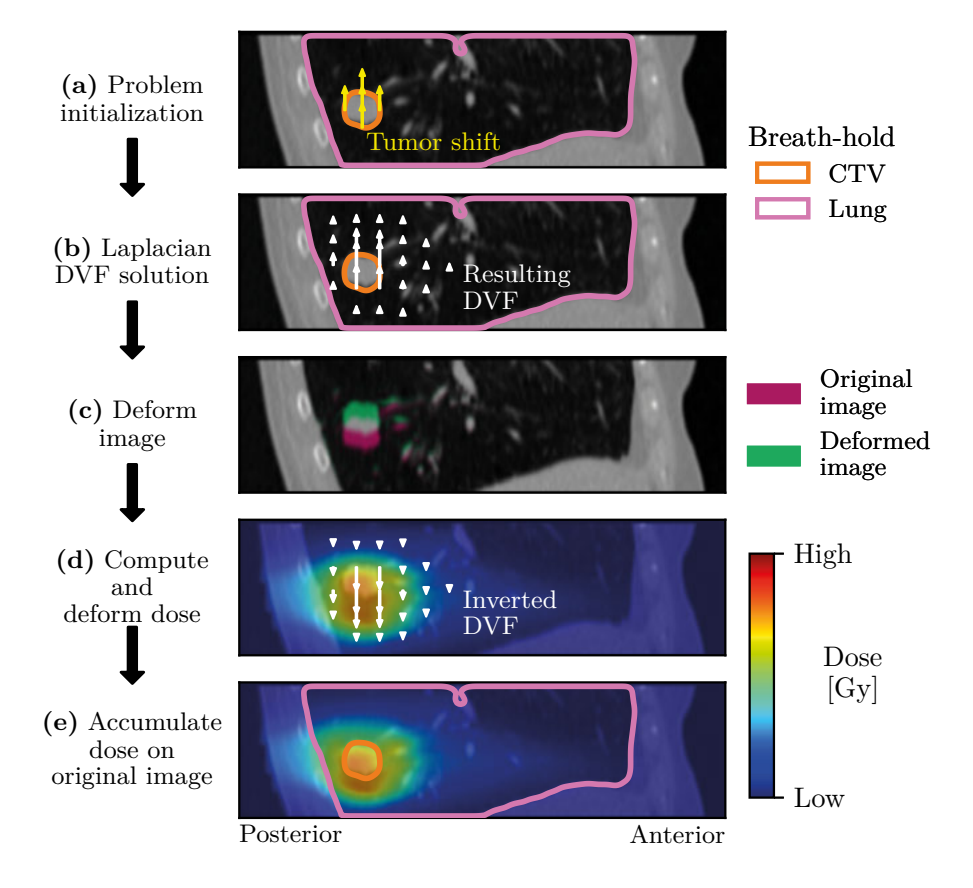


Figure 13. Breath-hold images for the probabilistic evaluation in paper V were created using a Laplacian deformation scheme introduced in paper III used to create displacement vector field (DVF) transforms. Shifts of the clinical target volume (CTV) were set according to the sampling method described in Figure 14 taking both systematic and per-BH reproducibility errors into account such that two sets of 105 BH images were created for each of the 14 patients in the cohort used in the studies of this thesis.

position were used both for treatment planning and, primarily, for treatment plan evaluations in the BH studies in paper V. The tumor shifts simulated the BH reproducibility error and were sampled at discrete positions according to their probability distribution as modeled with reported values for patients with advanced lung cancer (Josipovic et al., 2019; Hoffmann et al., 2023).

3.3 Simulation of treatment uncertainties

In paper I only the effects of respiratory motion were investigated. In papers II - V other treatment uncertainties were also simulated.

Since only the systematic patient positioning errors were simulated in paper II, larger shifts were used and sampled at 15 positions including the zero shift. The length of all non-zero shifts were 5 mm, set to match the 5 mm PTV margin and the 5 mm shifts used in the robust optimized treatment plans. Probabilities for the shifts were computed from an isotropic 3D normal distribution and used as weights in the probabilistic treatment plan evaluations.

The simulation methods developed in paper III and further used in papers IV and V were also based on discrete samples of errors but now divided into systematic and random components. Patient positioning errors were computed at two possible confidence intervals from the 3D normal distributions assumed during treatment planning (W. Li et al., 2011). The positioning errors of the tumor due to BH reproducibility uncertainty (Josipovic et al., 2019; Hoffmann et al., 2023) were similarly sampled as discrete shifts and used in the evaluation image creation for the BH investigations. All positioning errors were associated with a probability computed with a method similar to the one used in paper II, see Figure 14. However, this improved method was not limited to isotropic normal distributions such that the standard deviations could be different along the three principal axes, left-right (LR), anteriorposterior (AP), and craniocaudal (CC), as is typically the case in the reported values of these uncertainties, as seen in Table 2. These probabilities were used when sampling treatment scenario dose distributions in the probabilistic treatment plan evaluations performed in papers III - V. Finally, errors in SPR (B. Li et al., 2017) were sampled at three positions, as seen in Figure 15, and added to the simulations for the proton therapy plans with probabilities calculated from a 1D normal distribution. A summary of the uncertainties considered is found in Table 2.

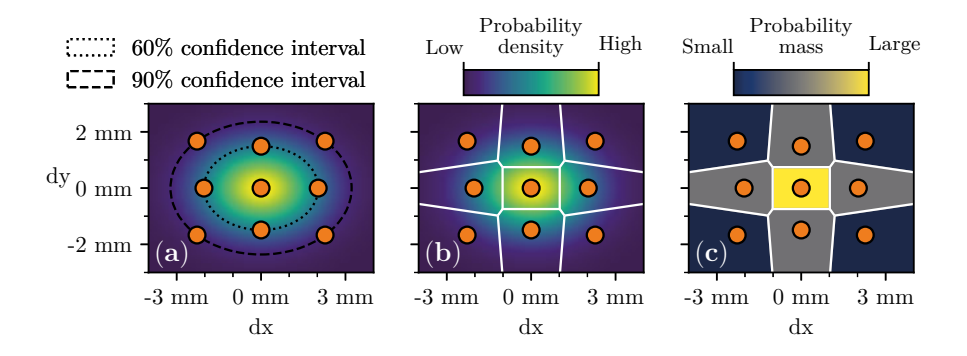


Figure 14. Positioning errors in patient positioning and BH reproducibility were modeled with zero-centered normal distributions, here visualized in 2D. Discrete errors used in the probabilistic evaluations in papers III - V were sampled at one or two confidence levels (a). Probability density (b) was integrated into a probability mass (c) that determined the likelihood of each discrete error.

Table 2. Standard deviations or source for the parameters of the perturbations used in the robust planning and evaluation. Σ refers to systematic errors that persist during the whole treatment and σ to random errors that are different at each fraction or breath-hold. The positional standard deviations are given in the left-right (LR), anterior-posterior (AP), and craniocaudal (CC) directions. Patient setup error in paper II was backwards modeled from the 5 mm PTV margin employed at the Uppsala university hospital.

	LR	AP	CC
Patient setup positioning [mm] (W. Li et al., 2011) (papers III - V)			
$\Sigma_{ ext{PS}}$	1.1	1.5	1.4
σ_{PS}	1.4	1.7	1.7
Breath-hold tumor position [mm] (Josipovic et al., 2019) (papers III ar	nd V)		
$\Sigma_{ m BH ext{-}J}$	1.3	1.2	1.1
$\sigma_{ m BH-J}$	0.9	1.0	1.0
Breath-hold tumor position [mm] (Hoffmann et al., 2023) (paper V)			
$\Sigma_{ ext{BH-H}}$	1.0	1.2	2.2
$\sigma_{ m BH-H}$	1.1	1.6	2.7
Free-breathing tumor positions (Wikström et al., 2021) (papers I - IV)			
		cine-CT	1
Stopping power ratio (B. Li et al., 2017) (papers III - V)			
$\Sigma_{ m SPR}$		3.8 %	

3.4 Robust and probabilistic evaluation

A robustness evaluation of a treatment plan is performed by subjecting the plan to various perturbations such as shifts in patient position and recomputing the dose (Goitein, 1985). The dose can further be recomputed on different image sets to allow for changes in, or motion of the internal anatomy. Since no computationally demanding plan optimization is taking place during the evaluation a higher number of different perturbations can be used than is typically considered during robust optimization. Dose metrics for the perturbed dose distributions are calculated and reported.

A probabilistic evaluation is done by performing the very same calculations for similar scenarios, but the perturbations are weighted by or sampled according to a probability distribution. This is a more realistic way of simulating treatments since the errors are assumed and modeled as probabilistic in nature with their standard deviations reported, see Table 2. Further, it permits a probabilistic interpretation of the results.

In paper I a robust evaluation based on recomputing the treatment plans on all the cine-CT derived evaluation images were used to compare four treatment planning methods. As no positioning errors were considered in the study none were used in the evaluation. Further, no splitting of the cine-CT image data

according to the three imaging occasions was performed, leading to a single evaluation dose per patient and treatment plan. This evaluation dose was used to calculate dose metrics in the CTV while all other dose metrics were reported for the nominal, unperturbed, dose distribution.

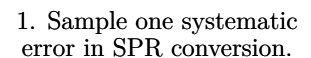
In paper II the dose was recomputed on the same evaluation images as in paper I but now split according to the three cine-CT imaging occasions, labeled as A, B, and C as seen in Figure 15. Further, probability weighted patient shifts that simulated systematic patient positioning errors were applied at discrete positions, as described in Section 3.3. All possible scenarios according to these discrete positioning error samples and with the evaluation images split into three sets were combinatorically explored. This resulted in 16 215 probability weighted evaluation doses per patient and treatment plan which equaled 227 010 evaluation doses in total per treatment planning method. However, because of the limitations in the evaluation image method no such scenarios were simulated for the OARs and thus the nominal dose distributions were used in the treatment plan comparisons, just as in paper I.

The probabilistic evaluation method developed in paper III added further methodological improvements by splitting the positioning errors into systematic and *random* components that could be sampled from non-isotropic normal distributions. Further, the DVF editing method allowed for full dose accumulation outside of the CTV which permitted a probabilistic evaluation of the dose in all OARs. The method used for the FB proton treatment plan evaluations is illustrated in Figure 15. The analogous method for the BH treatment plans was similar but with additional steps for the systematic and per-BH errors in tumor position reproducibility. These methods were used in the evaluation of the treatment plans in papers IV and V. In both, 10 000 treatment scenario dose distributions were sampled per patient and treatment plan which equaled 140 000 evaluation dose distributions in total per treatment planning method.

In practice all of these evaluations were performed by exporting perturbed dose distributions from the treatment planning system and storing them for retrospective evaluation and analysis. A summary of the treatment plan evaluation methods used in this thesis is found in Table 3.

Table 3. Treatment plan evaluation methods used throughout the thesis. The effects of respiratory motion were evaluated in all papers. *The treatments plans in paper I did not include setup uncertainty. \dagger Paper III only reported results for a single patient.

	Photon only		Photon and proton		
	I*	II	III^{\dagger}	IV	V
Robust evaluation					
(Respiratory motion only)	•				
Probabilistic evaluation					
(Systematic errors only)		'			
Probabilistic evaluation			./	./	./
(Systematic and <i>random</i> errors)			'	'	v



- 2. Sample one systematic patient positioning error.
- 3. Sample one patient positioning error for each treatment fraction.
- 4. Sample one set of evaluation images per fraction, corresponding to the breathing pattern at that occasion.
- 5. Compute fraction dose distributions by recomputing the plan on the evaluation image sets with applied errors in SPR and positioning and computing the averaged dose distribution.
- 6. Compute the scenario dose distribution as the sum of the three fraction dose distributions.

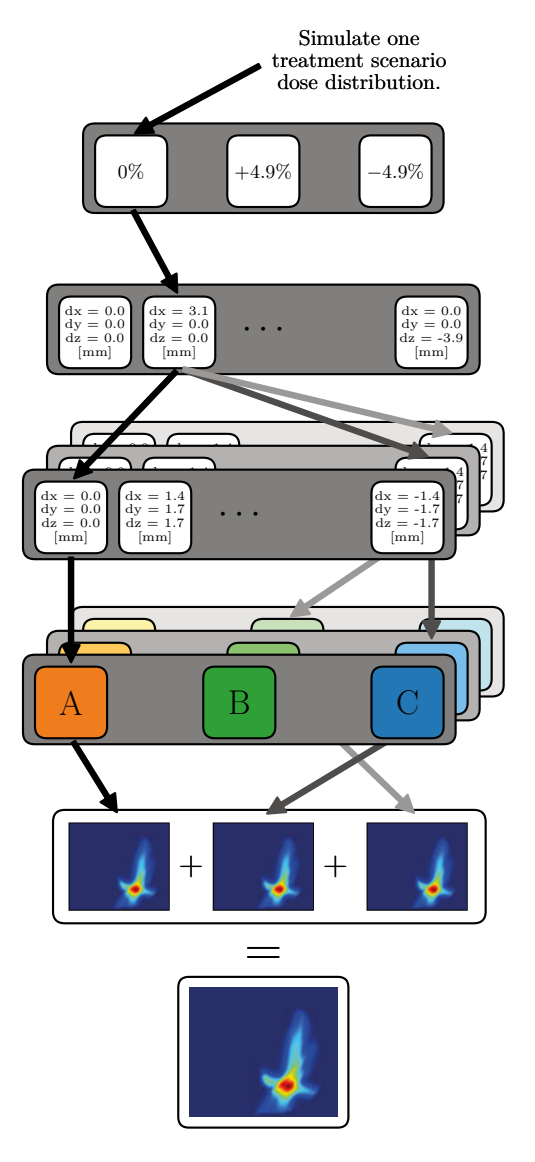


Figure 15. The probabilistic evaluation of the free-breathing (FB) proton plans in papers III and IV was performed by sampling preset, discrete, errors in stopping power ratio (SPR), systematic and fraction-wise patient positioning, as well as one of the three sets of cine-CT based evaluation images. In total 10 000 such treatment scenario dose distributions were simulated for each patient and FB treatment plan. The BH treatments simulated in paper V used an analogous method for sampling simulated treatments which is illustrated in paper III. In paper II a simpler approach that only simulated a larger systematic positioning error was used.

4. Results and discussion

4.1 Evaluation summaries and reporting

For all the multiple evaluation scenario dose distributions, dose metrics and DVHs were computed. The multiple DVHs were summarized into DVH bands that represented the total range of the DVH values in the evaluation. The individual dose metrics were all represented by distributions ranging from a minimal and a maximum value, both corresponding to two distinct evaluation dose distributions, as illustrated for the CTV $D_{50\%}$ in Figure 16. The number of samples obtained and analyzed varied across the studies reported in papers I - V as described in Section 3.4 and depended on whether the evaluation concerned the CTV or the OARs.

In the following subsections, results containing only one single evaluation dose distribution per patient are shown as box plots while the results from the probabilistic evaluations containing the results from many simulated evaluation dose distributions are shown as violin plots. In Figures 17, 18, 19, and 20 the scatter plotted data points represent the results for the individual patients and are connected with gray lines between the plots. The results for the patient used as example throughout this thesis report, patient number 2 shown e.g. in Figure 16, are shown as slightly larger black crosses connected by a black line. In the case of a box plot the data points represent the singular value for the individual patients while in the case of a violin plot the data points represent percentiles for which 90% of the cases are above, in the case of CTV target coverage evaluation, or 90% of the cases are below, in the case of OAR dose.

4.2 Target coverage

The CTV dose volume metrics were computed for the scenario doses and in particular the CTV $D_{50\%}$ was reported for all treatment plans investigated in this thesis. The resulting evaluation CTV $D_{50\%}$ distributions summarized for all 14 patients for all treatment plans investigated in this thesis in papers I - V, except some variations on the BH treatment plans found in paper V, can be seen in Figure 17.

4.3 Dose to the ipsilateral lung

Because of the rigid tumor registration in the evaluation image creation the ipsilateral lung dose for the evaluation process was not properly defined in

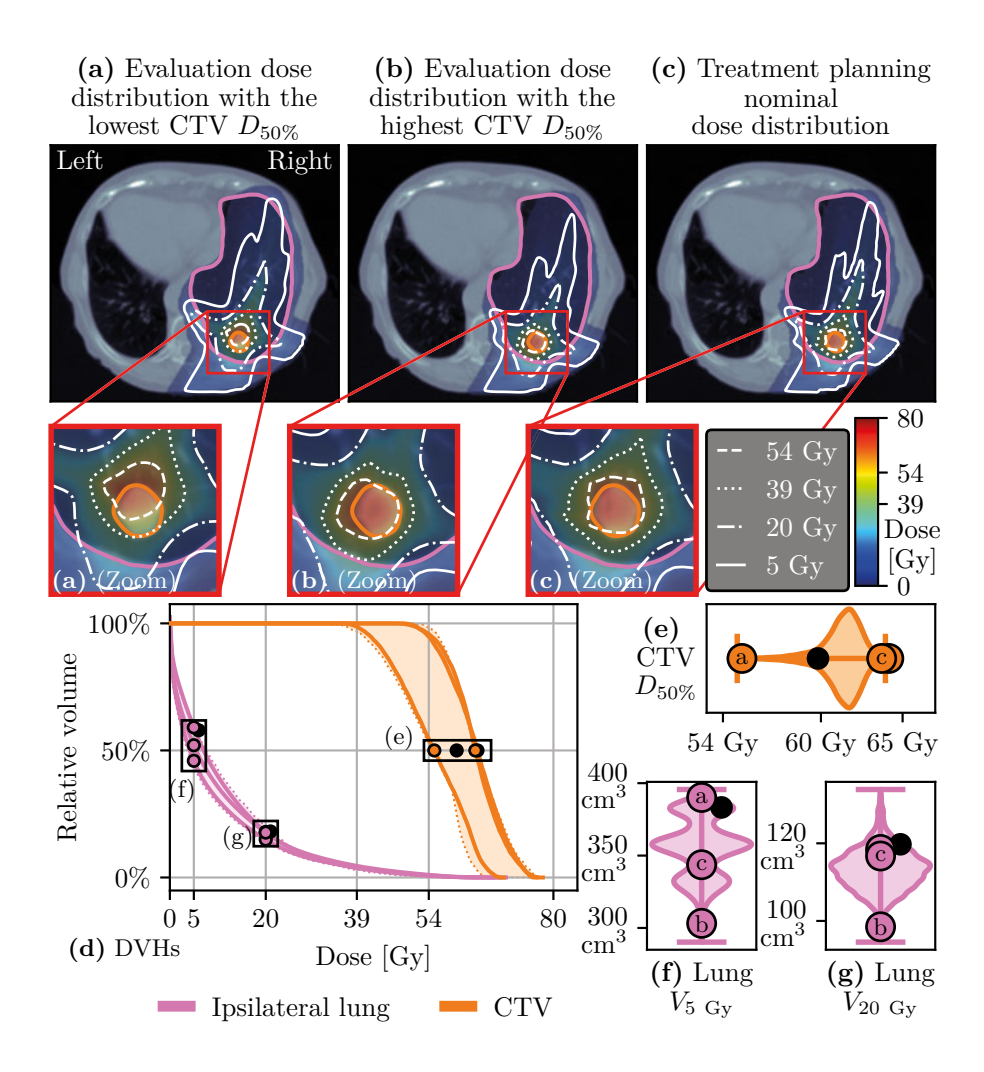


Figure 16. By subjecting the treatment plan to patient shifts, using the evaluation image sets, and applying a perturbation to the stopping power ratio (SPR) evaluation dose distributions, dose volume histograms (DVH), and dose metrics were computed. The evaluation dose distributions with the lowest (a) and highest (b) resulting clinical target volume (CTV) $D_{50\%}$ are shown for a free-breathing (FB) proton plan together with the nominal plan dose distribution in (c). The resulting evaluation DVHs (d) will thus create a range of such curves that in papers I and II were summarized as dose volume coverage and in papers III - V were used to determine curves of iso-probability. The resulting dose metrics will create ranges of values, seen for CTV $D_{50\%}$ in (e), lung $V_{5 \text{ Gy}}$ in (f), and lung $V_{20 \text{ Gy}}$ in (g). The DVH curves and the dose metric values corresponding to the three dose distributions in (a), (b), and (c) are indicated in (d), (e), (f), and (g). The values for which 90% of the cases were above, for CTV $D_{50\%}$, or below, for lung $V_{5 \text{ Gy}}$ and $V_{20 \text{ Gy}}$, are indicated by the black dots in (d), (e), (f), and (g) and were horizontally offset for the lung metrics for the purpose of visibility.

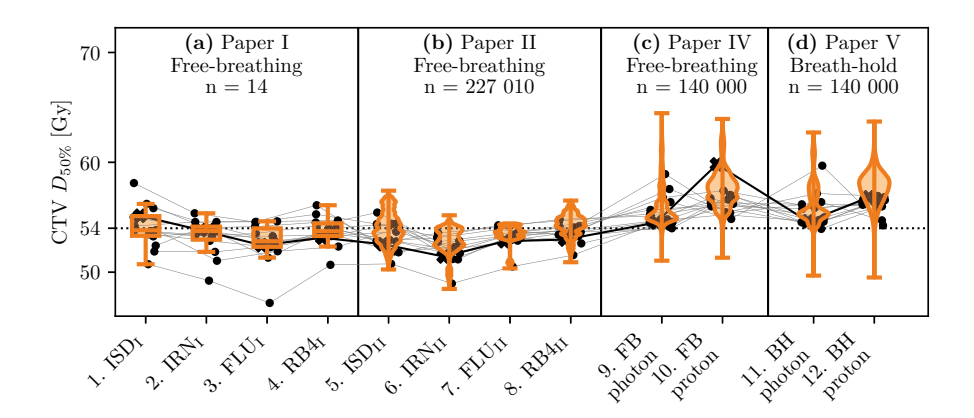


Figure 17. Evaluation clinical target volume (CTV) $D_{50\%}$ distribution results for the treatment plans investigated in this thesis. The scatter plotted data points represent the results for the individual patients and are connected with gray lines between the plots. The patient used as example throughout this thesis report and also shown e.g. in Figure 16 is shown as slightly larger black crosses connected by a black line. The prescription dose of CTV $D_{50\%} = 54$ Gy is shown with a dotted line.

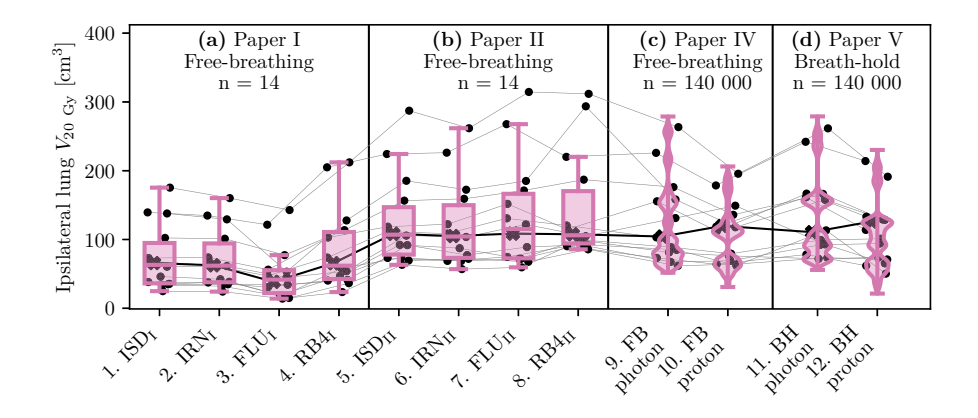


Figure 18. Evaluation ipsilateral lung $V_{20~\rm Gy}$ distribution results for the treatment plans investigated in this thesis. The values reported for papers I and II are the non-perturbed, nominal values. Note that the reason that the resulting $V_{20~\rm Gy}$ values were much lower for the treatment plans investigated in paper I is that they were planned without consideration for patient setup errors. Unlike the results for papers II, IV, and V they do therefore not represent clinically viable plans. The scatter plotted data points represent the results for the individual patients and are connected with gray lines between the plots. The patient used as example throughout this thesis report and also shown e.g. in Figure 16 is shown as slightly larger black crosses connected by a black line.

papers I and II. Therefore the ipsilateral lung doses were compared between the planning methods using the nominal plan dose computed on the 4DCT 30% phase image. Further, since the entire lung volumes were not visible in the CT images, volume-at-dose were computed in absolute terms and reported in cm³ for the dose metrics $V_{20~\rm Gy}$ and $V_{5~\rm Gy}$, seen in Figures 18 and 19. The results for the studies in papers IV and V were reported for the probabilistic evaluation and thus contained 10 000 samples per patient and treatment planning method.

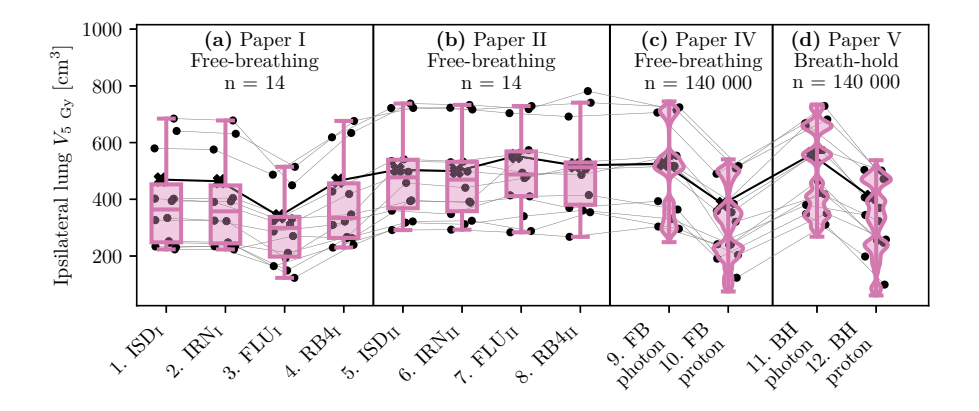


Figure 19. Evaluation ipsilateral lung $V_{5\,\mathrm{Gy}}$ distribution results for the treatment plans investigated in this thesis. The values reported for papers I and II are the non-perturbed, nominal values. Note that the reason that the resulting $V_{5\,\mathrm{Gy}}$ values were lower for the treatment plans investigated in paper I is that they were planned without consideration for patient setup errors. Unlike the results for papers II, IV, and V they do therefore not represent clinically viable plans. The scatter plotted data points represent the results for the individual patients and are connected with gray lines between the plots. The patient used as example throughout this thesis report and also shown e.g. in Figure 16 is shown as slightly larger black crosses connected by a black line.

4.4 Dose to mediastinal organs at risk (OARs)

Doses to the OARs primarily considered throughout this thesis were reported. The $D_{\rm mean}$ was reported for the heart and $D_{\rm max}$ for the aorta, esophagus, and the spinal cord shown for the FB photon, FB proton, and BH proton treatment planning methods in Figure 20. It should be noted that the entire heart was not visible on the CT images for any of the patients and for some it was not visible at all, for which a $D_{\rm mean}=0$ was reported.

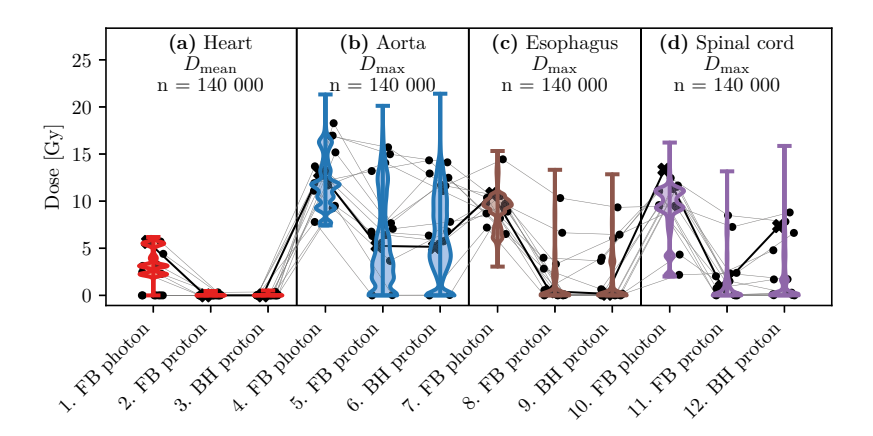


Figure 20. Evaluation distribution results of the dose to the included OARs for the FB photon, FB proton, and the BH proton treatment plans investigated in this thesis in papers IV and V. The scatter plotted data points represent the results for the individual patients and are connected with gray lines between the plots. The patient used as example throughout this thesis report and also shown e.g. in Figure 16 is shown as slightly larger black crosses connected by a black line.

4.5 Discussion

The results indicated an overall good target coverage for all treatment planning methods investigated, as seen in Figure 17.

The results for the treatment planning methods studied in papers I and II indicate that any planning method that use a dose computation algorithm suitable for heterogeneous media and takes the respiratory motion into account using 4D treatment planning will be reasonably robust with regards to target coverage. However, some variation in dose levels and inter-patient results are to be expected depending on the method chosen, as seen in Figure 17 (a) and (b). Especially it can be seen that the FLU_{II} method gave the most consistent inter-patient results while the RB4_{II} gave the overall highest CTV $D_{50\%}$ results for the study in paper II.

The systematically lower CTV $D_{50\%}$ value for one patient in papers I and II was not present in later studies since it was caused by a limitation in the evaluation image creation method that was improved in paper III.

The robust optimization perturbation settings calculated in paper III together with the robust evaluation and normalization step in the treatment planning used for papers IV and V resulted in a CTV $D_{50\%}$ that could be guaranteed to be above the prescribed dose level of 54 Gy with a 90% probability for both the photon and proton plans in FB and in BH. The greater variation in the results are to be expected for the studies in papers IV and V when compared with the ones in papers I and II since more types of and larger errors were simulated in the evaluations. The interpretation of this is that the robust optimization

method developed in paper III and used in these later studies was superior to the margin based and robust optimization treatment planning used in the earlier studies since the target coverage could be properly guaranteed at the desired confidence level.

Dose to the ipsilateral lung was reported in papers I and II. Both $V_{20~\rm Gy}$ and $V_{5~\rm Gy}$ was lower for FLU_I when compared with the other treatment planning methods in paper I, Figures 18 (a) and 19 (a). However, due to the increased field openings in the FLU_{II} this advantage for the fluence based treatment planning method did not persist in the study reported in paper II where the lung doses were very similar between the different treatment planning methods, Figures 18 (b) and 19 (b). It should be noted that the lung doses reported for paper I did not represent clinically viable values since no patient positioning uncertainty was considered in the treatment planning and evaluation of that particular study.

The vertical order of the patients, as seen by the lines drawn in Figures 18 and 19 are nearly constant. This is explained by the fact that dose to lung should be directly correlated to the size of the target which of course is the same regardless of treatment planning technique or treatment modality.

The doses to OARs were reduced with proton therapy compared with photon therapy, as seen in Figures 18, 19 and 20.

When comparing the FB proton with the FB photon and the BH proton with the BH photon it can be seen that both $V_{20~\rm Gy}$ and $V_{5~\rm Gy}$ was reduced with proton therapy, Figures 18 and 19 (c) and (d).

The $D_{\rm mean}$ for the heart was close to zero for both the FB and the BH proton planning methods as seen in Figure 20 (a). Although there were an overall reduction in $D_{\rm max}$ for the aorta, esophagus, and the spinal cord with proton therapy when compared with photon therapy, Figure 20 (b), (c), and (d), some patients had a higher risk of receiving a proton dose to these OARs. This risk is likely dependent on tumor location in relation to the OAR at hand. However, it should be noted that the 90th percentiles were mostly lower for these dose metrics for the proton therapy plans compared with the FB photon therapy plan and that all these values are well below the clinical constraints (Benedict et al., 2010; Timmerman, 2022).

The limited benefit of the BH treatment planning compared with the FB treatment planning as observed in Figure 17, 18, 19 and 20 is explained by the limited respiratory motion in many of the patients used in the studies. Although some of them demonstrated a very substantial FB motion many had tumor amplitudes below 10 mm as observed in the 4DCT, paper I. As such the simulated BH reproducibility tumor shifts derived from the population based uncertainties reported for advanced lung cancer patients resulted in larger irradiated volumes for the BH treatment plans compared with the FB treatment plans. However the target coverage and reduction in dose to OARs were still demonstrated for the BH proton plans when compared with photon therapy.

Target coverage and a reduction in dose to the OARs could be guaranteed with robust optimized proton therapy in either FB or BH when compared with photon therapy. These results demonstrate both the dosimetric advantages and the feasibility of proton therapy in the SBRT setting for small lung tumors.

5. Conclusions

Respiratory motion and other geometrical and radiological uncertainties and their management are a concern for lung cancer radiotherapy. Evaluating their impact on the clinical dose is important when comparing different treatment planning methods and modalities. This is of special importance in proton therapy as the effects of the uncertainties and any motion of the target are theoretically of greater dosimetric consequence.

Relying on the same 4DCT for both planning and evaluation is a limitation of many dosimetric studies since the 4DCT may not accurately represent the patients breathing during treatment. As reported in paper I, 4DCT underestimated the extent of the tumor motion for all patients in the cohort of 14 patients used in this thesis. In these studies, additional cine-CT imaging was used to better capture the true extent of the FB tumor motion and further used to create sets of evaluation images with two different methods developed in papers I and III. As part of the BH studies, the reproducibility uncertainty was simulated with tumor shifts and an image deformation method developed in paper III.

In papers I and II four different treatment planning methods for photon SBRT were investigated. The results indicated that any of the four methods give good target coverage. The best target coverage in these studies were achieved with robust optimization, $RB4_I$ and $RB4_{II}$, while the fluence based treatment planning, FLU_I and FLU_{II} , gave the most consistent intra-patient results and best dose homogeneity in the target. Further, the fluence based photon therapy treatment planning had the advantage of being the easiest and fastest method to practically implement out of all treatment planning methods investigated in this thesis.

Since PTV based treatment planning for proton is severely limited for small targets in the lungs robust optimization was further investigated in paper III. A method for calculating the perturbation settings for robust treatment planning of photon and proton plans in both FB and in BH was developed and a probabilistic evaluation method that used additional image deformations was proposed. The results in papers IV and V demonstrated that the proposed robust treatment planning method guaranteed target coverage at the desired confidence level.

Both 4D treatment planning, papers I - IV, and the use of BH, papers III and V, was investigated.

Finally, proton therapy demonstrated a substantial reduction in dose to the OARs. A reduction that could benefit all patients with lung cancer to be treated with SBRT.

6. Future perspectives and prospects

The treatment landscape for lung cancer has changed a lot since the introduction of SBRT in the 1990s and the treatment landscape for cancer in general has changed even more since the introduction of proton therapy in the 1950s.

The management of cancer no longer consists of just surgery, radiation therapy, and broad spectrum chemo therapies. The most important families of new therapies that have been introduced these past decades are targeted therapies such as immunotherapies, in the case of NSCLC primarily in the form of immune checkpoint inhibitors. This is a clear win for the patients as they in more cases than ever before can expect to be successfully treated and even cured of their disease than ever before. However it makes the life for clinicians and researchers that want to give their patients the very best treatments possible very challenging both when it comes to clinical decisions on which treatments to give and how clinical studies should be designed as all possible combinations of treatments are not possible to study in randomized clinical trials.

It is important to recognize that we should not expect any benefits in local control of the tumor for proton therapy compared with photon therapy. Any benefits observed will be from the reduced dose to healthy tissues and future clinical studies must therefore be designed with this in mind. It must further be recognized that not all patient groups will derive an observable benefit from this reduction in dose. Patients with local or distant recurrence will have a life expectancy directly related to the progress of recurring disease and will see no direct effects of the reduced dose to healthy tissues. However there are several ways that the reduced dose to healthy tissues with proton therapy could benefit these patients indirectly in subsequent treatments or in combination with other forms of treatment.

First of all we must recognize for which patients and how the current SBRT treatments fail. The most severe form of failure is distant metastases, this occurs in approximately 10% of the treated patients (Chi et al., 2010; Bradley et al., 2010; Senthi et al., 2012; Robinson et al., 2013; Tonneau et al., 2023; Sawayanagi et al., 2022). Distant metastases in general is outside the scope and purpose of SBRT to treat, however the reduced dose burden of proton therapy compared with photon therapy could bring benefits that are yet to be seen when combined with new systemic targeted therapies. One such modulator not explored in this thesis that has shown early promise is through the reduction of dose to the immune system which would give proton therapy an advantage when compared with photon therapy when combining SBRT with targeted immunotherapy (Zhang et al., 2023; Friedes et al., 2024). This has been

introduced in the common terminology of radiation therapy by treating the immune system as its own OAR or by using an immune system surrogate such as the blood. Combining immunotherapy with radiation therapy has been demonstrated for advanced lung cancer (Spigel et al., 2022). However, the complexity and hard to assess driving mechanisms that motivates combination therapies must be recognized, as must the way studies should be designed and reported (Daly, 2022; Van Aken et al., 2025; Phillips et al., 2025).

The other form of treatment failure is locoregional failure which is defined as a recurrence in the irradiated volume. These patients have been shown to be successfully treated by giving a second course of SBRT in the form of salvage therapy (Sun et al., 2017; Jang et al., 2025; Dähler et al., 2025). However this will of course lead to higher dose burden to all OARs compared with a single course of SBRT. Here there is an obvious benefit of proton therapy as much of the dose to all mediastinal OARs could be greatly reduced or even completely removed and a larger lung volume could be spared in the lower dose region, e.g. at the $V_{5\,\text{GV}}$ level (McAvoy et al., 2013).

The incidence of lung cancer in the Swedish population has fallen over the recent decades, likely because of a reduction in tobacco smoking and as people with an interest in treating lung cancer we remind ourselves that this is a good thing. However there has been a slight increase in the incidence in young women. Further, screening programmes for parts of the population at high risk are currently under investigation (Cancercentrum, 2025). Both of these would lead to younger people being diagnosed with their lung cancer while in early stage and could therefore be of interest to treat with SBRT. Younger and otherwise healthier people are also more likely to benefit from the long term benefits of a reduced dose to e.g. the heart and other OARs that proton therapy would provide as compared with photon therapy.

Due to the increasing precision with which radiation therapy can be delivered there has recently been an increasing interest in treating groups of patients that have previously not been treated with radiation therapy due to a heightened risk of adverse side effects.

One such patient group is those with central lung tumors, as opposed to the patients with peripheral lung tumors studied in this thesis (K. Lindberg et al., 2021; S. Lindberg et al., 2023; Yan et al., 2023). These patients have proven to be very difficult to treat both with radiation therapy and otherwise due to the location of the tumor being in the immediate neighborhood of the mediastinal OARs or the bronchus. As no effective treatments exist these patients have a very poor prognosis. Recently there have been clinical studies on the use of MR integrated radiation therapy, MR-linac, to treat these patients (Hoffmann et al., 2022). This special form of integrated imaging and treatment delivery allows for a great reduction in positioning uncertainty as well as improved respiratory management. However it is still limited to photon therapy and although integrated MR imaging and proton therapy exists at a research level it is still not available at the Skandion clinic in Uppsala. If it ever becomes

available as a clinically commercial solution it will be very expensive. However the dosimetric benefits of proton therapy could still be explored and compared with MR-linac for the central and ultra central lung tumor patient groups and the potential dosimetric benefits and downsides weighted for each modality.

Another patient group is those with oligometastatic disease that may or may not be from a primary lung tumor. In this setting SBRT is used as a middle ground of local and systemic therapy to treat several targets as part of one treatment course (Guckenberger et al., 2020; Kroeze et al., 2023; Tsai et al., 2024). Depending on the location of these metastases the dosimetric benefits of using proton therapy over photon therapy could be further enhanced by use of beam directions.

Proton therapy can be beneficial for all these newer and expanded patient groups as well as for the current patients treated with SBRT. The benefit for all these future patients will only ever be provided if we first dare to take the first steps in adopting proton therapy for SBRT. This thesis has demonstrated that we can proceed with confidence when using proton therapy even for SBRT of small lung tumors that are subjected to respiratory motion and other treatment related uncertainties as they can indeed be managed.

7. Sammanfattning på Svenska

Lung cancer är den globalt sett vanligaste orsaken till cancer-relaterad död och i Sverige så diagnostiseras 4500 nya fall per år. Prognosen för de flesta patienter är dålig men för de som diagnostiseras i tidigt stadie med en liten, väl avgränsad, lung cancer utan metastaser kan kurativ behandling med stereotaktisk precisionsstrålbehandling ge mycket god lokal kontroll av tumören. Precisionsstrålbehandling utmärks av de höga stråldoserna som ges vid ett fåtal, oftast tre till fem, behandlingstilfällen. Idag ges dessa behandlingar med högenergetisk Röntgenstrålning. Skulle dessa behandlingar istället kunna ges med protonstrålning så skulle de teoretiska dosimetriska fördelarna av bestrålning med laddade partiklar kunna nyttjas till att drastiskt reducera dosbördan på frisk vävnad. De första protonstrålbehandlingarna av cancer gjordes på 1950-talet i Uppsala. Sedan 2015 är modern protonstrålbehandling tillgängligt på Skandionkliniken i Uppsala men hittills har inga behandlingar av patienter med lung cancer och inga precisionsstrålbehandlingar utförts vilket denna avhandling adresserar.

När man behandlar lungtumörer är hanteringen av andningsrörelsen mycket viktig och flera olika tillvägagångssätt har utvecklats och implementerats kliniskt. I det här projektet har olika dosplaneringsmetoder för precisionsstrålbehandling som tar hänsyn till andningsrörelse utvärderats och jämförts. Vidare har metoder för dosplanering och utvärdering för precisionsstrålbehandling med protoner utvecklats. Särskilda bildtagningar med datortomografi och simuleringsstrategier användes för att undersöka de olika dosplaneringsmetoderna. Både behandlingar i friandning och under andningsuppehåll undersöktes.

Resultaten visar att robustplanerade behandlingar för den här patientgruppen ger en garanterad dos i tumören för både foton och protonbestrålning i både friandning och med andningsuppehåll. Vidare visar resultaten att strålbehandling med protoner skulle ge en stor minskning i bestrålning av frisk vävnad runt tumörområdet. Detta skulle ge dessa patienter en mer skonsam behandling om de behandlades med protonstrålbehandling så som denna avhandling förespråkar.

8. Acknowledgments

First I would like to thank all my supervisors. My main supervisor Alexandru and my most senior supervisor Anders. When I applied for this position I was sitting in a basement on the other side of the Atlantic ocean and I had just packed my bags to return home in defeat. It was in the middle of the night not many hours before my flight would leave and it was also the last day the application would be open. In all honesty I did not know a whole lot about radiation therapy and either I succeeded in fooling you that I did or you saw through it and decided I would still be a good candidate for this project. Either way I am grateful that you granted me this opportunity.

I would also like to thank Kenneth for his in practice closer supervision of this project. Without the work you had done during your own thesis nothing of what I have worked on would have been possible.

I want to thank everyone at the radiotherapy department. Especially David, Nina, Erik and Samuel for sharing the office and for the company at conferences and meetings.

I want to thank the subterranean people at the departments of nuclear medicine and diagnostic imaging for the lunches. A special thanks to Karolina. I feel like we were both equally surprised when we met each other at the writing course, *another physicist!*?.

I would like to thank all the people at IGP I have interacted with. A special thank you to Bo for among other things allowing me to both take and teach courses. A second special thank you to Maria at the economic administration for helping me with all my issues and applications. Thank you to Eleftherios, Mehran, Tianqi, Hanna and the other radioactive people.

Thank you to the current and former members of the IGP student council but especially to Ale and Tiarne (and/or Bea?) for organizing the first IGP PhD student conference I attended.

Thank you to Berta and Tabassom for starting and organizing the cancer precision journal clubs. Most of the time I understood very little but if you just try to say something that sounds smart you can fool almost anyone, even yourself.

I want to thank all my students. It has been a privilege to teach you and I hope you have learned as much from me as I have from you. A special thank you to "my" master students Sewa and Katharine.

I want to thank all my friends for dragging me outside. Björken Mattias for doing what I could not. Daniel for all the conversations. Åke Mattias for staying young at heart. Snuskis and Henning for whenever we all see each

other. Petter for the occasional but long runs and both you and Ashkan for the surprising timing of offspring. Gustav for calling and talking about the old days.

A thank you to the internet people. Kiddo, jotta (and his annihilated feet), OB, snuffe, snaka, doed, piccolo, kletet, natur, care, and kaktus for being our manager.

Les gens d'une autres fois, merci. Peut-être un jour.

Tack till min familj. Mamma och pappa för all hjälp. Alla mina bröder, Karl, Magnus, Henrik, Aron och Axel.

Och till sist tack Iris för att du orkat med hela vägen och förhoppningsvis mycket längre än bara hit.

A special thanks to Valeria for informing me of were I am allowed to sit, typically not were I want to, and were the raisins are kept in my own kitchen. How else would I get stomach flu if it was not for you.

9. Bibliography

- Ahnesjö, A. (1989). Collapsed cone convolution of radiant energy for photon dose calculation in heterogeneous media: Photon dose calculation. *Medical Physics*, 16(4), 577–592. https://doi.org/10.1118/1.596360
- Andreo, P. (1991). Monte Carlo techniques in medical radiation physics. *Physics in Medicine and Biology*, *36*(7), 861–920. https://doi.org/10.1088/0031-9155/36/7/001
- Aznar, M. C., Carrasco De Fez, P., Corradini, S., Mast, M., McNair, H., Meattini, I., Persson, G., & Van Haaren, P. (2023). ESTRO-ACROP guideline: Recommendations on implementation of breath-hold techniques in radiotherapy. *Radiotherapy and Oncology*, *185*, 109734. https://doi.org/10.1016/j.radonc.2023.109734
- Barnea, D. I., & Silverman, H. F. (1972). A Class of Algorithms for Fast Digital Image Registration. *IEEE Transactions on Computers*, *C-21*(2), 179–186. https://doi.org/10.1109/TC.1972.5008923
- Battista, J. (2019). *Introduction to megavoltage X-ray dose computations algorithms.* CRC Press. ISBN: 978-1-315-16511-0 978-1-351-67613-7.
- Baumann, R., Chan, M. K., Pyschny, F., Stera, S., Malzkuhn, B., Wurster, S., Huttenlocher, S., Szücs, M., Imhoff, D., Keller, C., Balermpas, P., Rades, D., Rödel, C., Dunst, J., Hildebrandt, G., & Blanck, O. (2018). Clinical results of mean GTV dose optimized robotic-guided stereotactic body radiation therapy for lung tumors. *Frontiers in Oncology*, 8. https://doi.org/10.3389/fonc.2018.00171
- Benedict, S. H., Yenice, K. M., Followill, D., Galvin, J. M., Hinson, W., Kavanagh, B., Keall, P., Lovelock, M., Meeks, S., Papiez, L., Purdie, T., Sadagopan, R., Schell, M. C., Salter, B., Schlesinger, D. J., Shiu, A. S., Solberg, T., Song, D. Y., Stieber, V., ... Yin, F. F. (2010). Stereotactic body radiation therapy: The report of AAPM Task Group 101. *Medical Physics*, 37(8), 4078–4101. https://doi.org/10.1118/1.3438081
- Bibault, J. E., Mirabel, X., Lacornerie, T., Tresch, E., Reynaert, N., & Lartigau, E. (2015). Adapted prescription dose for monte carlo algorithm in lung SBRT: Clinical outcome on 205 patients. *PLoS ONE*, *10*(7), 1–10. https://doi.org/10.1371/journal.pone.0133617
- Blomgren, H., Lax, I., Näslund, I., & Svanström, R. (1995). Stereotactic High Dose Fraction Radiation Therapy of Extracranial Tumors Using An Accelerator: Clinical experience of the first thirty-one patients. *Acta Oncologica*, *34*(6), 861–870. https://doi.org/10.3109/02841869509127197

- Bortfeld, T., & Schlegel, W. (1996). An analytical approximation of depth-dose distributions for therapeutic proton beams. *Physics in Medicine & Biology*, *41*(8), 1331–1339. https://doi.org/10.1088/0031-9155/41/8/006
- Bradley, J. D., El Naqa, I., Drzymala, R. E., Trovo, M., Jones, G., & Denning, M. D. (2010). Stereotactic Body Radiation Therapy for Early-Stage Non–Small-Cell Lung Cancer: The Pattern of Failure Is Distant. *International Journal of Radiation Oncology Biology Physics*, 77(4), 1146–1150. https://doi.org/10.1016/j.ijrobp.2009.06.017
- Brandan, M., Gregoire, V., & Howell, R. W. (2014). ICRU Report 91 Prescribing, Recording, and Reporting of Stereotactic Treatments with Small Photon Beams. *Journal of the ICRU*, *14*(2). https://doi.org/10.1093/jicru/ndx017
- Bray, F., Laversanne, M., Sung, H., Ferlay, J., Siegel, R. L., Soerjomataram, I., & Jemal, A. (2024). Global cancer statistics 2022: GLOBOCAN estimates of incidence and mortality worldwide for 36 cancers in 185 countries. *CA: A Cancer Journal for Clinicians*, 74(3), 229–263. https://doi.org/10.3322/caac.21834
- Bush, K., Gagne, I. M., Zavgorodni, S., Ansbacher, W., & Beckham, W. (2011). Dosimetric validation of Acuros® XB with Monte Carlo methods for photon dose calculations. *Medical Physics*, *38*(4), 2208–2221. https://doi.org/10.1118/1.3567146
- Buti, G., Souris, K., Montero, A. M. B., Lee, J. A., & Sterpin, E. (2019). Towards fast and robust 4D optimization for moving tumors with scanned proton therapy. *Medical Physics*, 46(12), 5434–5443. https://doi.org/10.1002/mp.13850
- C. Joiner, M. (2025). *Basic Clinical Radiobiology* (6th ed) [Chapter 14, page 156]. Taylor & Francis Group. ISBN: 978-1-032-24381-8 978-1-040-19436-2.
- Cancercentrum. (2025). Nationellt vårdprogram lungcancer 2025. https://cancercentrum.se/utvecklingsarbeteutbildning/statistikrapporter/rapporter. 657.html
- Cancerfonden. (2023). Cancerfonden Strålbehandling. Retrieved January 16, 2023, from https://www.cancerfonden.se/om-cancer/behandlingar/stralbehandling
- Chi, A., Liao, Z., Nguyen, N. P., Xu, J., Stea, B., & Komaki, R. (2010). Systemic review of the patterns of failure following stereotactic body radiation therapy in early-stage non-small-cell lung cancer: Clinical implications. *Radiotherapy and Oncology*, 94(1), 1–11. https://doi.org/10.1016/j.radonc.2009.12.008
- D E Raeside. (1976). Monte Carlo principles and applications. *Physics in Medicine & Biology*, 21(2), 181–197. https://doi.org/10.1088/0031-9155/21/2/001

- Dähler, K., Day, M., Kefer, K., Torelli, N., Von Der Grün, J., Joye, A., Mayinger, M. C., Tanadini-Lang, S., Balermpas, P., Guckenberger, M., Andratschke, N., & Willmann, J. (2025). Evaluation of the prognostic value of the ESTRO/EORTC classification of reirradiation in patients with nonsmall cell lung cancer. *Radiotherapy and Oncology*, *210*, 111003. https://doi.org/10.1016/j.radonc.2025.111003
- Daly, M. E. (2022). Inoperable Early-Stage Non–Small-Cell Lung Cancer: Stereotactic Ablative Radiotherapy and Rationale for Systemic Therapy. *Journal of Clinical Oncology*, *40*(6), 539–545. https://doi.org/10.1200/JCO.21.01611
- Darby, S. C., Ewertz, M., McGale, P., Bennet, A. M., Blom-Goldman, U., Brønnum, D., Correa, C., Cutter, D., Gagliardi, G., Gigante, B., Jensen, M.-B., Nisbet, A., Peto, R., Rahimi, K., Taylor, C., & Hall, P. (2013). Risk of Ischemic Heart Disease in Women after Radiotherapy for Breast Cancer. *New England Journal of Medicine*, *368*(11), 987–998. https://doi.org/10.1056/NEJMoa1209825
- de Jong, E. E., Guckenberger, M., Andratschke, N., Dieckmann, K., Hoogeman, M. S., Milder, M., Møller, D. S., Nyeng, T. B., Tanadini-Lang, S., Lartigau, E., Lacornerie, T., Senan, S., Verbakel, W., Verellen, D., De Kerf, G., & Hurkmans, C. (2020). Variation in current prescription practice of stereotactic body radiotherapy for peripherally located early stage non-small cell lung cancer: Recommendations for prescribing and recording according to the ACROP guideline and ICRU report 91. *Radiotherapy and Oncology*, 142, 217–223. https://doi.org/10.1016/j. radonc.2019.11.001
- Falkmer, S., Fors, B., Larsson, B., Lindell, A., Naeslund, J., & Stenson, S. (1962). Pilot Study on Proton Irradiation of Human Carcinoma. *Acta Radiologica*, *58*(1), 33–51. https://doi.org/10.3109/00016926209169546
- Fogliata, A., Nicolini, G., Clivio, A., Vanetti, E., & Cozzi, L. (2011). Dosimetric evaluation of Acuros XB Advanced Dose Calculation algorithm in heterogeneous media. *Radiation Oncology*, *6*(1), 82. https://doi.org/10.1186/1748-717X-6-82
- Ford, E. C., Mageras, G. S., Yorke, E., & Ling, C. C. (2003). Respiration-correlated spiral CT: A method of measuring respiratory-induced anatomic motion for radiation treatment planning. *Medical Physics*, 30(1), 88–97. https://doi.org/10.1118/1.1531177
- Fredriksson, A., Forsgren, A., & Hårdemark, B. (2011). Minimax optimization for handling range and setup uncertainties in proton therapy. *Medical Physics*, *38*(3), 1672–1684. https://doi.org/10.1118/1.3556559
- Friedes, C., Iocolano, M., Lee, S. H., Duan, L., Li, B., Doucette, A., Cohen, R. B., Aggarwal, C., Sun, L. L., Levin, W. P., Cengel, K. A., Kao, G., Teo, B.-K. K., Langer, C. J., Xiao, Y., Bradley, J., Feigenberg, S. J., & Yegya-Raman, N. (2024). The effective radiation dose to immune cells predicts lymphopenia and inferior cancer control in

- locally advanced NSCLC. *Radiotherapy and Oncology*, *190*, 110030. https://doi.org/10.1016/j.radonc.2023.110030
- Goitein, M. (1985). Calculation of the uncertainty in the dose delivered during radiation therapy. *Medical Physics*, 12(5), 608–612. https://doi.org/10. 1118/1.595762
- Goitein, M., Wittenberg, J., Mendiondo, M., Doucette, J., Friedberg, C., Ferrucci, J., Gunderson, L., Linggood, R., Shipley, W. U., & Fineberg, H. V. (1979). The value of ct scanning in radiation therapy treatment planning: A prospective study. *International Journal of Radiation Oncology Biology Physics*, *5*(10), 1787–1798. https://doi.org/10.1016/0360-3016(79)90562-5
- Gregoire, V., Mackie, T. R., De Neve, W., Gospodarowicz, M., van Herk, M., & Niemierko, A. (2010). ICRU Report 83 Prescribing, recording, and reporting photon-beam intensity-modulated radiation therapy (IMRT). *Journal of the ICRU*, *10*(1). https://doi.org/10.1093/jicru\ ndq002
- Guckenberger, M., Andratschke, N., Dieckmann, K., Hoogeman, M. S., Hoyer, M., Hurkmans, C., Tanadini-Lang, S., Lartigau, E., Méndez Romero, A., Senan, S., & Verellen, D. (2017). ESTRO ACROP consensus guideline on implementation and practice of stereotactic body radiotherapy for peripherally located early stage non-small cell lung cancer. *Radiotherapy and Oncology*, *124*(1), 11–17. https://doi.org/10.1016/j.radonc. 2017.05.012
- Guckenberger, M., Lievens, Y., Bouma, A. B., Collette, L., Dekker, A., deSouza, N. M., Dingemans, A.-M. C., Fournier, B., Hurkmans, C., Lecouvet, F. E., Meattini, I., Méndez Romero, A., Ricardi, U., Russell, N. S., Schanne, D. H., Scorsetti, M., Tombal, B., Verellen, D., Verfaillie, C., & Ost, P. (2020). Characterisation and classification of oligometastatic disease: A European Society for Radiotherapy and Oncology and European Organisation for Research and Treatment of Cancer consensus recommendation. *The Lancet Oncology*, *21*(1), e18–e28. https://doi.org/10.1016/S1470-2045(19)30718-1
- Hanley, J., Mageras, G. S., Mychalczak, B., Gloeggler, P. J., & Leibel, S. A. (1999). Deep inspiration breath-hold technique for lung tumors: The potential value of target immobilization and reduced lung density in dose escalation. *International Journal of Radiation Oncology Biology Physics*, 45(3). https://doi.org/10.1016/S0360-3016(99)00154-6
- Hoffmann, L., Persson, G., Nygård, L., Nielsen, T., Borrisova, S., Gaard-Petersen, F., Josipovic, M., Khalil, A., Kjeldsen, R., Knap, M., Kristiansen, C., Møller, D., Ottosson, W., Sand, H., Thing, R., Pøhl, M., & Schytte, T. (2022). Thorough design and pre-trial quality assurance (QA) decrease dosimetric impact of delineation and dose planning variability in the STRICTLUNG and STARLUNG trials for stereotactic body radiotherapy (SBRT) of central and ultra-central lung tumours.

- Radiotherapy and Oncology, 171, 53–61. https://doi.org/10.1016/j.radonc.2022.04.005
- Hoffmann, L., Ehmsen, M., Hansen, J., Hansen, R., Knap, M., Mortensen, H., Poulsen, P., Ravkilde, T., Rose, H., Schmidt, H., Worm, E., & Møller, D. (2023). Repeated deep-inspiration breath-hold CT scans at planning underestimate the actual motion between breath-holds at treatment for lung cancer and lymphoma patients. *Radiotherapy and Oncology*, *188*, 109887. https://doi.org/10.1016/j.radonc.2023.109887
- Holmqvist, M., & Wagenius, G. (2024). Lungcancer Nationell kvalitetsrapport för 2023. https://cancercentrum.se/utvecklingsarbeteutbildning/statistikrapporter/rapporter/rapporter/lungcancernationellkvalitetsrapportfor2023. 1363.html
- Jang, K., Cross, S., & Yeghiaian-Alvandi, R. (2025). Stereotactic Reirradiation for In-Field Lung Cancer Recurrence after Stereotactic Ablative Radiotherapy: A Systematic Review and Meta-Analysis. *Radiotherapy* and Oncology, 208. https://doi.org/10.1016/j.radonc.2025.110898
- Josipovic, M., Aznar, M. C., Thomsen, J. B., Scherman, J., Damkjaer, S. M., Nygård, L., Specht, L., Pøhl, M., & Persson, G. F. (2019). Deep inspiration breath hold in locally advanced lung cancer radiotherapy: Validation of intrafractional geometric uncertainties in the INHALE trial. *The British Journal of Radiology*, 92(1104), 20190569. https://doi.org/10.1259/bjr.20190569
- Kang, Y., Zhang, X., Chang, J. Y., Wang, H., Wei, X., Liao, Z., Komaki, R., Cox, J. D., Balter, P. A., Liu, H., Zhu, X. R., Mohan, R., & Dong, L. (2007). 4D Proton treatment planning strategy for mobile lung tumors. *International Journal of Radiation Oncology Biology Physics*, 67(3), 906–914. https://doi.org/10.1016/j.ijrobp.2006.10.045
- Keall, P. J., Mageras, G. S., Balter, J. M., Emery, R. S., Forster, K. M., Jiang, S. B., Kapatoes, J. M., Low, D. A., Murphy, M. J., Murray, B. R., et al. (2006). The management of respiratory motion in radiation oncology report of AAPM Task Group 76 a. *Medical physics*, 33(10), 3874–3900. https://doi.org/10.1118/1.2349696
- Khalil, A. A., Hoffmann, L., Moeller, D. S., Farr, K. P., & Knap, M. M. (2015). New dose constraint reduces radiation-induced fatal pneumonitis in locally advanced non-small cell lung cancer patients treated with intensity-modulated radiotherapy. *Acta Oncologica*, *54*(9), 1343–1349. https://doi.org/10.3109/0284186X.2015.1061216
- Kroeze, S. G. C., Pavic, M., Stellamans, K., Lievens, Y., Becherini, C., Scorsetti, M., Alongi, F., Ricardi, U., Jereczek-Fossa, B. A., Westhoff, P., But-Hadzic, J., Widder, J., Geets, X., Bral, S., Lambrecht, M., Billiet, C., Sirak, I., Ramella, S., Giovanni Battista, I., ... Guckenberger, M. (2023). Metastases-directed stereotactic body radiotherapy in combination with targeted therapy or immunotherapy: Systematic review and consensus recommendations by the EORTC–ESTRO OligoCare

- consortium. *The Lancet Oncology*, 24(3), e121–e132. https://doi.org/10.1016/S1470-2045(22)00752-5
- Langen, K., & Zhu, M. (2018). Concepts of PTV and Robustness in Passively Scattered and Pencil Beam Scanning Proton Therapy. *Seminars in Radiation Oncology*, 28(3), 248–255. https://doi.org/10.1016/j.semradonc.2018.02.009
- Larsson, B., Lidén, K., & Sarby, B. (1974). Irradiation of Small Structures Through the Intact Skull [Publisher: Informa UK Limited]. *Acta Radiologica: Therapy, Physics, Biology, 13*(6), 512–534. https://doi.org/10.3109/02841867409132650
- Lawrence, J. H. (1957). Proton irradiation of the pituitary. *Cancer*, *10*(4), 795–798. https://doi.org/10.1002/1097-0142(195707/08)10:4<795::AID-CNCR2820100426>3.0.CO;2-B
- Lax, I., Blomgren, H., Näslund, I., & Svanström, R. (1994). Stereotactic Radiotherapy of Malignancies in the Abdomen: Methodological aspects. *Acta Oncologica*, *33*(6), 677–683. https://doi.org/10.3109/02841869409121782
- Lebredonchel, S., Lacornerie, T., Rault, E., Wagner, A., Reynaert, N., & Crop, F. (2017). About the non-consistency of PTV-based prescription in lung. *Physica Medica*, *44*, 177–187. https://doi.org/10.1016/j.ejmp. 2017.03.009
- Leung, R. W. K., Chan, M. K. H., Chiang, C. L., Wong, M., & Blanck, O. (2020). On the pitfalls of PTV in lung SBRT using type-B dose engine: An analysis of PTV and worst case scenario concepts for treatment plan optimization [Publisher: Radiation Oncology ISBN: 1301402001]. *Radiation Oncology*, *15*(1), 1–16. https://doi.org/10.1186/s13014-020-01573-9
- Li, B., Lee, H. C., Duan, X., Shen, C., Zhou, L., Jia, X., & Yang, M. (2017). Comprehensive analysis of proton range uncertainties related to stopping-power-ratio estimation using dual-energy CT imaging. *Physics in Medicine & Biology*, 62(17), 7056–7074. https://doi.org/10.1088/1361-6560/aa7dc9
- Li, H., Dong, L., Bert, C., Chang, J., Flampouri, S., Jee, K.-W., Lin, L., Moyers, M., Mori, S., Rottmann, J., Tryggestad, E., & Vedam, S. (2022). AAPM Task Group Report 290: Respiratory motion management for particle therapy. *Medical Physics*, 49(4). https://doi.org/10.1002/mp.15470
- Li, W., Purdie, T. G., Taremi, M., Fung, S., Brade, A., Cho, B. J., Hope, A., Sun, A., Jaffray, D. A., Bezjak, A., & Bissonnette, J.-P. (2011). Effect of Immobilization and Performance Status on Intrafraction Motion for Stereotactic Lung Radiotherapy: Analysis of 133 Patients. *International Journal of Radiation Oncology Biology Physics*, 81(5), 1568–1575. https://doi.org/10.1016/j.ijrobp.2010.09.035

- Li, X.-J., Ye, Y.-C., Zhang, Y.-S., & Wu, J.-M. (2022). Empirical modeling of the percent depth dose for megavoltage photon beams (S. Hashim, Ed.). *PLoS ONE*, *17*(1). https://doi.org/10.1371/journal.pone.0261042
- Lindberg, K., Grozman, V., Karlsson, K., Lindberg, S., Lax, I., Wersäll, P., Persson, G. F., Josipovic, M., Khalil, A. A., Moeller, D. S., Nyman, J., Drugge, N., Bergström, P., Olofsson, J., Rogg, L. V., Ramberg, C., Kristiansen, C., Jeppesen, S. S., Nielsen, T. B., ... Lewensohn, R. (2021). The HILUS-Trial—a Prospective Nordic Multicenter Phase 2 Study of Ultracentral Lung Tumors Treated With Stereotactic Body Radiotherapy. *Journal of Thoracic Oncology*, *16*(7), 1200–1210. https://doi.org/10.1016/j.jtho.2021.03.019
- Lindberg, S., Grozman, V., Karlsson, K., Onjukka, E., Lindbäck, E., Jirf, K. A., Lax, I., Wersäll, P., Persson, G. F., Josipovic, M., Khalil, A. A., Møller, D. S., Hoffmann, L., Knap, M. M., Nyman, J., Drugge, N., Bergström, P., Olofsson, J., Rogg, L. V., ... Lindberg, K. (2023). Expanded HILUS Trial: A Pooled Analysis of Risk Factors for Toxicity From Stereotactic Body Radiation Therapy of Central and Ultracentral Lung Tumors. *International Journal of Radiation Oncology Biology Physics*, 117(5), 1222–1231. https://doi.org/10.1016/j.ijrobp.2023.06.246
- Liu, W., Feng, H., Taylor, P. A., Kang, M., Shen, J., Saini, J., Zhou, J., Giap, H. B., Yu, N. Y., Sio, T. S., Mohindra, P., Chang, J. Y., Bradley, J. D., Xiao, Y., Simone, C. B., & Lin, L. (2024). NRG Oncology and Particle Therapy Co-Operative Group Patterns of Practice Survey and Consensus Recommendations on Pencil-Beam Scanning Proton Stereotactic Body Radiation Therapy and Hypofractionated Radiation Therapy for Thoracic Malignancies. *International Journal of Radiation Oncology Biology Physics*, 119(4), 1208–1221. https://doi.org/10.1016/j.ijrobp. 2024.01.216
- McAvoy, S. A., Ciura, K. T., Rineer, J. M., Allen, P. K., Liao, Z., Chang, J. Y., Palmer, M. B., Cox, J. D., Komaki, R., & Gomez, D. R. (2013). Feasibility of proton beam therapy for reirradiation of locoregionally recurrent non-small cell lung cancer. *Radiotherapy and Oncology*, 109(1), 38–44. https://doi.org/10.1016/j.radonc.2013.08.014
- Nakajima, K., Oguri, M., Iwata, H., Hattori, Y., Hashimoto, S., Nomura, K., Hayashi, K., Toshito, T., Akita, K., Baba, F., Ogino, H., & Hiwatashi, A. (2024). Long-term survival outcomes and quality of life of image-guided proton therapy for operable stage I non-small cell lung cancer: A phase 2 study. *Radiotherapy and Oncology*, *196*, 110276. https://doi.org/10.1016/j.radonc.2024.110276
- Paganetti, H. (Ed.). (2019). *Proton therapy physics* (Second edition) [Chapter 1.4.3 "Current Clinical Implications"]. CRC Press. ISBN: 978-1-351-85574-7 978-1-351-85575-4 978-1-351-85573-0.
- Paganetti, H., Blakely, E., Carabe-Fernandez, A., Carlson, D. J., Das, I. J., Dong, L., Grosshans, D., Held, K. D., Mohan, R., Moiseenko, V., Niemierko,

- A., Stewart, R. D., & Willers, H. (2019). Report of the AAPM TG -256 on the relative biological effectiveness of proton beams in radiation therapy. *Medical Physics*, 46(3). https://doi.org/10.1002/mp.13390
- Paganetti, H., Niemierko, A., Ancukiewicz, M., Gerweck, L. E., Goitein, M., Loeffler, J. S., & Suit, H. D. (2002). Relative biological effectiveness (RBE) values for proton beam therapy. *International Journal of Radiation Oncology Biology Physics*, *53*(2), 407–421. https://doi.org/10.1016/S0360-3016(02)02754-2
- Perez, P., Gangnet, M., & Blake, A. (2003). Poisson image editing. *ACM Transactions on Graphics*, 22(3), 313–318. https://doi.org/10.1145/882262.882269
- Phillips, W. J., Jackson, A., Kidane, B., Lim, G., Navani, V., & Wheatley-Price, P. (2025). Immunotherapy for Early-Stage Non–Small Cell Lung Cancer: A Practical Guide of Current Controversies. *Clinical Lung Cancer*, 26(3), 179–190. https://doi.org/10.1016/j.cllc.2025.01.006
- Robinson, C. G., DeWees, T. A., El Naqa, I. M., Creach, K. M., Olsen, J. R., Crabtree, T. D., Meyers, B. F., Puri, V., Bell, J. M., Parikh, P. J., & Bradley, J. D. (2013). Patterns of Failure after Stereotactic Body Radiation Therapy or Lobar Resection for Clinical Stage I Non–Small-Cell Lung Cancer. *Journal of Thoracic Oncology*, 8(2), 192–201. https://doi.org/10.1097/JTO.0b013e31827ce361
- Rueckert, D. (1999). Nonrigid registration using free-form deformations: Application to breast mr images. *IEEE Transactions on Medical Imaging*, 18(8), 712–721. https://doi.org/10.1109/42.796284
- Sawayanagi, S., Yamashita, H., Nozawa, Y., Takenaka, R., Miki, Y., Morishima, K., Ueno, H., Ohta, T., & Katano, A. (2022). Establishment of a Prediction Model for Overall Survival after Stereotactic Body Radiation Therapy for Primary Non-Small Cell Lung Cancer Using Radiomics Analysis. *Cancers*, 14(16), 3859. https://doi.org/10.3390/cancers14163859
- Schwarz, M., Cattaneo, G. M., & Marrazzo, L. (2017). Geometrical and dosimetrical uncertainties in hypofractionated radiotherapy of the lung: A review. *Physica Medica*, *36*, 126–139. https://doi.org/10.1016/j.ejmp. 2017.02.011
- Senthi, S., Lagerwaard, F. J., Haasbeek, C. J., Slotman, B. J., & Senan, S. (2012). Patterns of disease recurrence after stereotactic ablative radiotherapy for early stage non-small-cell lung cancer: A retrospective analysis. *The Lancet Oncology*, *13*(8), 802–809. https://doi.org/10.1016/S1470-2045(12)70242-5
- Seppenwoolde, Y., Shirato, H., Kitamura, K., Shimizu, S., van Herk, M., Lebesque, J. V., & Miyasaka, K. (2002). Precise and real-time measurement of 3D tumor motion in lung due to breathing and heartbeat, measured during radiotherapy. *International Journal of Radiation Oncology Biology Physics*, *53*(4), 822–834. https://doi.org/10.1016/S0360-3016(02)02803-1

- Sorkine, O., Cohen-Or, D., Lipman, Y., Alexa, M., Rössl, C., & Seidel, H.-P. (2004). Laplacian surface editing. *Proceedings of the 2004 Eurographics/ACM SIGGRAPH symposium on Geometry processing*, 175–184. ISBN: 978-3-905673-13-5https://doi.org/10.1145/1057432.1057456
- Sotiras, A., Davatzikos, C., & Paragios, N. (2013). Deformable medical image registration: A survey. *IEEE Transactions on Medical Imaging*, *32*(7), 1153–1190. https://doi.org/10.1109/TMI.2013.2265603
- Spigel, D. R., Faivre-Finn, C., Gray, J. E., Vicente, D., Planchard, D., Paz-Ares, L., Vansteenkiste, J. F., Garassino, M. C., Hui, R., Quantin, X., Rimner, A., Wu, Y.-L., Özgüroğlu, M., Lee, K. H., Kato, T., De Wit, M., Kurata, T., Reck, M., Cho, B. C., ... Antonia, S. J. (2022). Five-Year Survival Outcomes From the PACIFIC Trial: Durvalumab After Chemoradiotherapy in Stage III Non–Small-Cell Lung Cancer. *Journal of Clinical Oncology*, 40(12), 1301–1311. https://doi.org/10.1200/JCO. 21.01308
- Sun, B., Brooks, E. D., Komaki, R., Liao, Z., Jeter, M., McAleer, M., Balter, P. A., Welsh, J. D., O'Reilly, M., Gomez, D., Hahn, S. M., Sepesi, B., Rice, D. C., Heymach, J. V., & Chang, J. Y. (2017). Long-Term Outcomes of Salvage Stereotactic Ablative Radiotherapy for Isolated Lung Recurrence of Non–Small Cell Lung Cancer: A Phase II Clinical Trial. *Journal of Thoracic Oncology*, 12(6), 983–992. https://doi.org/10.1016/j.jtho.2017.02.018
- Timmerman, R. (2022). A Story of Hypofractionation and the Table on the Wall. *International Journal of Radiation Oncology Biology Physics*, 112(1), 4–21. https://doi.org/10.1016/j.ijrobp.2021.09.027
- Tonneau, M., Richard, C., Routy, B., Campeau, M.-P., Vu, T., Filion, E., Roberge, D., Mathieu, D., Doucet, R., Beliveau-Nadeau, D., & Bahig, H. (2023). A competing risk analysis of the patterns and risk factors of recurrence in early-stage non-small cell lung cancer treated with stereotactic ablative radiotherapy. *Radiotherapy and Oncology*, *185*, 109697. https://doi.org/10.1016/j.radonc.2023.109697
- Tsai, C. J., Yang, J. T., Shaverdian, N., Patel, J., Shepherd, A. F., Eng, J., Guttmann, D., Yeh, R., Gelblum, D. Y., Namakydoust, A., Preeshagul, I., Modi, S., Seidman, A., Traina, T., Drullinsky, P., Flynn, J., Zhang, Z., Rimner, A., Gillespie, E. F., ... Zhi, W. (2024). Standard-of-care systemic therapy with or without stereotactic body radiotherapy in patients with oligoprogressive breast cancer or non-small-cell lung cancer (Consolidative Use of Radiotherapy to Block [CURB] oligoprogression): An open-label, randomised, controlled, phase 2 study. *The Lancet*, 403(10422), 171–182. https://doi.org/10.1016/S0140-6736(23)01857-3
- Unkelbach, J., Alber, M., Bangert, M., Bokrantz, R., Chan, T. C., Deasy, J. O., Fredriksson, A., Gorissen, B. L., Van Herk, M., Liu, W., Mahmoudzadeh, H., Nohadani, O., Siebers, J. V., Witte, M., & Xu, H.

- (2018). Robust radiotherapy planning. *Physics in Medicine & Biology*, 63(22). https://doi.org/10.1088/1361-6560/aae659
- Van Aken, E. S., Devnani, B., Castelo-Branco, L., De Ruysscher, D., Martins-Branco, D., Marijnen, C. A., Muoio, B., Belka, C., Lordick, F., Kroeze, S., Pentheroudakis, G., Trapani, D., Ricardi, U., Gandhi, A. K., Prelaj, A., O'Cathail, S. M., & De Jong, M. C. (2025). ESMO-ESTRO framework for assessing the interactions and safety of combining radiotherapy with targeted cancer therapies or immunotherapy [Publisher: Elsevier BV]. *Radiotherapy and Oncology*, 208, 110910. https://doi.org/10.1016/j.radonc.2025.110910
- Van Herk, M., Remeijer, P., Rasch, C., & Lebesque, J. V. (2000). The probability of correct target dosage: Dose-population histograms for deriving treatment margins in radiotherapy. *International Journal of Radiation Oncology Biology Physics*, 47(4), 1121–1135. https://doi.org/10.1016/S0360-3016(00)00518-6
- Vedam, S. S., Keall, P. J., Kini, V. R., Mostafavi, H., Shukla, H. P., & Mohan, R. (2003). Acquiring a four-dimensional computed tomography dataset using an external respiratory signal. *Physics in Medicine & Biology*, 48(1), 45–62. https://doi.org/10.1088/0031-9155/48/1/304
- von Reibnitz, D., Shaikh, F., Wu, A. J., Treharne, G. C., Dick-Godfrey, R., Foster, A., Woo, K. M., Shi, W., Zhang, Z., Din, S. U., Gelblum, D. Y., Yorke, E. D., Rosenzweig, K. E., & Rimner, A. (2018). Stereotactic body radiation therapy (SBRT) improves local control and overall survival compared to conventionally fractionated radiation for stage I non-small cell lung cancer (NSCLC). *Acta Oncologica*, *57*(11), 1567–1573. https://doi.org/10.1080/0284186X.2018.1481292
- Wikström, K. A., Isacsson, U. M., Pinto, M. C., Nilsson, K. M., & Ahnesjö, A. (2021). Evaluation of irregular breathing effects on internal target volume definition for lung cancer radiotherapy. *Medical Physics*, 48(5), 2136–2144. https://doi.org/10.1002/mp.14824
- Willett, C. G., Linggood, R. M., Stracher, M. A., Goitein, M., Doppke, K., Kushner, D. C., Morris, T., Pardy, J., & Carroll, R. (1987). The effect of the respiratory cycle on mediastinal and lung dimensions in Hodgkin's disease. Implications for radiotherapy gated to respiration. *Cancer*, 60(6), 1232–1237. https://doi.org/10.1002/1097-0142(19870915)60: 6<1232::AID-CNCR2820600612>3.0.CO;2-F
- Wilson, R. R. (1946). Radiological Use of Fast Protons. *Radiology*, 47(5), 487–491. https://doi.org/10.1148/47.5.487
- Withers, H. R. (1975). The Four R's of Radiotherapy. In *Advances in Radiation Biology* (pp. 241–271, Vol. 5). Elsevier. ISBN: 978-0-12-035405-4https: //doi.org/10.1016/B978-0-12-035405-4.50012-8
- Wolthaus, J. W., Sonke, J. J., van Herk, M., Belderbos, J. S., Rossi, M. M., Lebesque, J. V., & Damen, E. M. (2008). Comparison of Different Strategies to Use Four-Dimensional Computed Tomography in Treat-

- ment Planning for Lung Cancer Patients. *International Journal of Radiation Oncology Biology Physics*, 70(4), 1229–1238. https://doi.org/10.1016/j.ijrobp.2007.11.042
- Yan, M., Louie, A. V., Kotecha, R., Ashfaq Ahmed, M., Zhang, Z., Guckenberger, M., Kim, M.-S., Lo, S. S., Scorsetti, M., Tree, A. C., Sahgal, A., & Slotman, B. J. (2023). Stereotactic body radiotherapy for Ultra-Central lung Tumors: A systematic review and Meta-Analysis and International Stereotactic Radiosurgery Society practice guidelines. *Lung Cancer*, 182, 107281. https://doi.org/10.1016/j.lungcan.2023.107281
- Zhang, W., Li, S., Zhang, C., Mu, Z., Chen, K., & Xu, Z. (2023). Tumor-infiltrating lymphocytes predict efficacy of immunotherapy in advanced non-small cell lung cancer: A single-center retrospective cohort study. *Acta Oncologica*, *62*(8), 853–860. https://doi.org/10.1080/0284186X. 2023.2228991

Acta Universitatis Upsaliensis

Digital Comprehensive Summaries of Uppsala Dissertations from the Faculty of Medicine 2169

Editor: The Dean of the Faculty of Medicine

A doctoral dissertation from the Faculty of Medicine, Uppsala University, is usually a summary of a number of papers. A few copies of the complete dissertation are kept at major Swedish research libraries, while the summary alone is distributed internationally through the series Digital Comprehensive Summaries of Uppsala Dissertations from the Faculty of Medicine. (Prior to January, 2005, the series was published under the title "Comprehensive Summaries of Uppsala Dissertations from the Faculty of Medicine".)



Distribution: publications.uu.se urn:nbn:se:uu:diva-564488